INTERNATIONAL JOURNAL OF ROBUST AND NONLINEAR CONTROL

Int. J. Robust. Nonlinear Control 0000; **00**:1–35

Published online in Wiley InterScience (www.interscience.wiley.com). DOI: 10.1002/rnc

On Distributed Reactive Power and Storage Control on Microgrids

Andres Cortés and Sonia Martínez[†]

SUMMARY

This manuscript develops a dual decomposition algorithm for the distributed control of reactive power and charging/discharging rates in microgrids with distributed solar generation and storage capacities. Our setting considers physical constraints inherent to storage systems and voltage regulation constraints with the objective of minimizing a cost function that encompasses two aspects: the total cost of the active power consumed by the microgrid and its associated transmission losses over a finite time horizon. We provide a complete analysis of the convergence of the proposed algorithm and introduce a novel approach for the distributed approximation of the voltage prediction over the power grid. Simulations demonstrate the performance of the dual decomposition algorithm on a particular microgrid case. Copyright © 0000 John Wiley & Sons, Ltd.

Received ...

KEY WORDS: Microgrid control, reactive power control, distributed optimization, battery control, MPC

[†]A. Cortés and S. Martínez are with Department of Mechanical and Aerospace Engineering, University of California, San Diego,9500 Gilman Drive La Jolla, CA 92093-0411{aicortes@ucsd.edu, soniamd@soe.ucsd.edu}.

1. INTRODUCTION

In a world with an increasing energy demand, solar energy stands as an important alternative that can partly replace the more limited fossil fuels or the riskier nuclear energy sources. However, as with other renewables, the high variability of solar irradiance makes its penetration into the energy mix very challenging. In order to solve problems related to voltage stability and variable load satisfaction, several solutions are being contemplated. Additional backup generation plants could help compensate fluctuations, but their deployment would incur significantly higher costs for both the utilities and the users. Large-scale storage systems are proposed to shift the energy generated during low-demand hours or that corresponding to high-solar generation times to those of high demand. Smart inverters placed at the PV themselves can be leveraged to inject reactive power for voltage regulation and optimization of the network performance. In particular, since PV systems and batteries can be locally owned and distributed throughout the network, distributed optimization algorithms can be used to achieve the power network objectives in a faster and more robust way. These objectives can be, to some extent, expressed as the well known *Optimal Power Flow* (OPF) problem.

The OPF problem [1] is a non-convex, hard optimization problem that has received wide attention in the literature. Most of the works on the OPF propose centralized solutions that consider voltage as a decision variable [2, 3]. Recently, the papers [3, 4, 5] circumvent the nonconvexity of the OPF through a relaxation that ensures a zero-duality gap under some general conditions. The work [6, 7] studies an OPF setting with storage integration in which battery systems are added to some nodes in a grid. The paper [6] addresses an OPF problem where voltages and battery charging/discharging rates are taken as decision variables, simplified by assumptions such as small-angles and infinite charging/discharging capacities. Electricity prices are assumed to vary over time, and the objective function is the cost of the energy provided by the utility. The paper [7] presents a more general setting in

Prepared using rncauth.cls
DOI: 10.1002/rnc

which the assumptions of [6] are avoided and exploits the aforementioned zero-duality-gap approach.

The reactive power control problem, which consists of providing for losses without producing excess heating or incurring voltage drops, has been addressed in a significant number of works. In the 1980s, banks of capacitors and transformer taps were used for reactive power compensation. In [8] a problem of optimal sizing for capacitors is solved using a relaxation of the power flow equations over radial networks. An optimal reactive power generation algorithm is introduced in [9], in order to minimize active power losses and improve voltage regulation. More recently, research has focused on the control of smart inverters which allow changes in the generated reactive power. In [10], a convexification of the OPF problem is presented for grids that fulfill some assumptions on the input voltage and the impedance in the transmission lines. The objective is to minimize transmission losses in the grid by varying the injected reactive power at all generators in a distributed way. This work does not consider voltage regulation constrains, which are addressed in [11]. Although the convexification idea of [11] remains identical to that of [10], a different communication structure is employed.

Here, we propose an algorithm to compute both the optimal reactive power generation and storage control strategies for a microgrid over a given time horizon. This computation is intended for use in a model-predictive control scheme that can incorporate forecasts on generation and load. In order to present a distributed algorithm based on the dual decomposition method, we employ a convexification approach that exploits high voltages at the connection point of the microgrid. The type of microgrid we consider is endowed with generation and/or storage capacity at certain nodes. We consider a discrete-time horizon, which, at each instant of time, has an associated electricity cost per kWh, a forecasted active generation, and node-wise load. The algorithm utilizes measurements and predictions of voltage in the microgrid, which have implicit information on the power injected at the nodes, in order to choose the optimal reactive power that must be injected by each generator,

Prepared using rncauth.cls
DOI: 10.1002/rnc

and the optimal charging/discharging rate of the storage at each node. The goal is to minimize a cost function that weighs in the grid transmission losses with the overall cost of the active power provided by the utility during the time horizon. Finally, the solution provided by the algorithm is meant to respect voltage regulation constraints. The present paper extends the work presented in [12]. The algorithm convergence analysis is performed by characterizing the behavior of an upper bound algorithm which can be studied via Lyapunov theory. In particular, we conclude that trajectories converge to the unique value of reactive power injection and charging/discharging rate for each node of the microgrid. Finally, we describe a novel way of approximately predicting voltage in order to implement the proposed algorithm.

This work is organized as follows. Section 2 presents the microgrid model and the optimization problem we aim to solve. Section 3 describes the dual decomposition algorithm to solve the optimization problem. Section 4 introduces a solution to voltage prediction required by the algorithm. Simulations are presented in Section 5 and Section 6 presents conclusions.

Short List of Notations.

T: Length of the optimization horizon

$\tau = \{1, \ldots, T\}$: Optimization horizon (set of time slots)

$\mathcal{G}$: Set of nodes with generation

$\mathcal{M}$: Set of nodes with load only

$p_{\text{load},\mathcal{A}}(t)$: Vector of active power of the loads for all nodes in the set $\mathcal{A} \subseteq \mathcal{V}$, $t \in \tau$

$p_{\text{in},\mathcal{G}}(t)$: Active power generated at all nodes in $\mathcal{G}$, $t \in \tau$

$q_{\text{load},\mathcal{A}}(t)$: Reactive power load for all nodes in $\mathcal{A} \subseteq \mathcal{V}$, $t \in \tau$

$q_{\text{in},\mathcal{G}}(t)$: Reactive power generated at all nodes in $\mathcal{G}$, $t \in \tau$

Prepared using rncauth.cls
DOI: 10.1002/rnc

$v(t)$: Control for batteries at all nodes in $\mathcal{G}$, for $t \in \tau$

β_l: Battery capacity for the l^{th} node , divided by length of each time slot in τ

$c(t)$: Active power cost per kWh at time $t \in \tau$

$u(t)$: Voltage at each node in $\mathcal{V}$, $t \in \tau$

$U_{\max}, U_{\min}$: Bounds on the voltage magnitude for nodes in $\mathcal{G}$

$\iota(t)$: Injected current at each node in $\mathcal{V}$, $t \in \tau$

$s(t)$: Injected complex power at each node in $\mathcal{V}$, $t \in \tau$

$\mathcal{N}_G(l)$: Neighbors of the node $l \in \mathcal{G}$ in the communication network

$V^l_{\text{ch}}, V^l_{\text{dis}}$: Bounds on the charged/discharged energy in the battery in node l at time $t \in \tau$

$\overline{\lambda}(t), \underline{\lambda}(t)$: Lagrange multipliers for the voltage constraints, $t \in \tau$

$\overline{\eta}(t), \underline{\eta}(t)$: Lagrange multipliers for charged/discharged energy constraints, $t \in \tau$

$\overline{\mu}(t), \underline{\mu}(t)$: Lagrange multipliers for constraints on the battery capacities, $t \in \tau$

1.1. Preliminary notation

In what follows, $\mathbb{R}$ will denote the set of real numbers, $\mathbb{R}_{>0}$ the set of real-positive numbers, $\mathbb{N}$ the set of natural numbers, and $\mathbb{C}$ the set of complex numbers. The complex exponential function is denoted as e^{jx}, for $x \in \mathbb{R}$. The notation $\|x\|$, for $x \in \mathbb{C}^n$ denotes the Euclidean norm of the vector x. The notation $\|X\|$, for $X \in \mathbb{C}^{m\times n}$, denotes the induced Euclidean norm of X, while $\|X\|_{\mathbb{C}} \in \mathbb{R}^{m\times n}_{\geq 0}$ is understood as an array whose entries are the magnitude of each entry of the variable $X \in \mathbb{C}^{m\times n}$ (for X scalar, vector or matrix). The operator $\angle X$ denotes the phase angle of all the complex entries of X. We let $\mathbf{e}_l \in \mathbb{R}^n$ be a vector whose $l+1$ entry is equal to one, for $l \in \{0, \ldots, n-1\}$, while all other entries are zero, and $\mathbf{1} \in \mathbb{R}^n$ be a vector which entries are all equal to one. Dimension of $\mathbf{e}_l$ and $\mathbf{1}$ depends on the context. The notation $\mathbf{0}_{m\times n} \in \mathbb{R}^{m\times n}$ represents a matrix whose entries are zero. Given the finite set $\mathcal{A}$, $|\mathcal{A}|$ denotes its cardinality. For $n \in \mathbb{N}$, I_n denotes the identity

Prepared using rncauth.cls
DOI: 10.1002/rnc

matrix in $\mathbb{R}^{n\times n}$. Consider a set $\tau = \{1,\dots,T\}$, and let $x \in \mathbb{C}^{|\mathcal{A}|T}$, with entries $x_l(t) \in \mathbb{C}$, for all $l \in \mathcal{A}$, $t \in \tau$; that is, $x = [x_1(1)\dots, x_{|\mathcal{A}|}(1),\dots, x_1(T),\dots, x_{|\mathcal{A}|}(T)]^\top$. Then, $x(t) \in \mathbb{C}^{|\mathcal{A}|}$ denotes the vector $x(t) = [x_1(t),\dots, x_{|\mathcal{A}|}(t)]^\top$, for each $t \in \tau$. Similarly, $x_l \in \mathbb{C}^\top$ denotes the vector $x_l = [x_l(1),\dots, x_l(T)]^\top$, for each $l \in \mathcal{A}$. For a complex square matrix A, we denote its spectrum as $\mathrm{spec}(A)$ and its spectral radius as $\rho(A)$. For the matrix A, A_{ij} represents its (i,j) entry. If A is block partitioned, $(A)_{ij}$ represents its (i,j) block. For $x \in \mathbb{C}^n$, $\mathbf{d}(x)$ denotes the diagonal matrix such that $\mathbf{d}(x)_{ii} = x_i$, for $i \in \{1,\dots,n\}$, while for a complex square matrix A, $\mathbf{d}(A)$ is a diagonal matrix such that $\mathbf{d}(A)_{ii} = A_{ii}$. Let C be a complex array in $\mathbb{C}^{m\times n}$, we denote the null space of C as $\mathrm{null}(C) \triangleq \{x \in \mathbb{C}^n \mid Cx = 0\}$. The row space of C, defined as the set of all linear combinations of the rows of C, is denoted as $\mathrm{row}(C)$. Finally, $\hat{C}$ denotes the conjugate transpose of C. Let $\mathcal{B} \subseteq \mathbb{R}^n$ be a convex set. Then, for $x \in \mathbb{R}^n$, $\mathrm{dist}(x,\mathcal{B}) \triangleq \inf_{y\in\mathcal{B}} \|x - y\|$. Given functions $f : \mathbb{R}^m \to \mathbb{R}$ and $g : \mathbb{R}^m \to \mathbb{R}^n$, we denote the "small-o" notation $g(x) = o\left(f(x)\right)$ if $\lim_{\|x\|\to\infty} g(x)f(x)^{-1} = 0$. For a vector $x \in \mathbb{R}^n$, $x \succeq 0$ indicates that all entries of x are nonnegative.

1.2. Notions of graph theory

Let $\mathbb{G} = (\mathcal{V}, \mathcal{E}, Y)$ be an undirected weighted graph with a set $\mathcal{V} = \{0,\dots,N-1\}$ of N vertices, a set of edges $\mathcal{E}$ and a symmetric weight matrix $Y \in \mathbb{C}^{N\times N}$. Each edge in $\mathcal{E}$ is expressed as (h,l), for $h,l \in \mathcal{V}$. Consider some labeling of the set $\mathcal{E}$ with the set of indices $\{1,\dots,|\mathcal{E}|\}$. In addition, let us assign an arbitrary direction to each edge $(h,l) \in \mathcal{E}$. The *incidence matrix* A of $\mathbb{G}$ is a matrix in $\{0,\pm1\}^{|\mathcal{E}|\times N}$, which depends on the arbitrary direction associated with each edge of $\mathbb{G}$, such that:

$$A_{dl} = \begin{cases} -1, & \text{if } \varepsilon_d \in \mathcal{E} \text{ is an outgoing edge of } l \in \mathcal{V}, \\ 1, & \text{if } \varepsilon_d \in \mathcal{E} \text{ is an incoming edge of } l \in \mathcal{V}, \\ 0, & \text{otherwise.} \end{cases}$$

Prepared using rncauth.cls
DOI: 10.1002/rnc

Consider a diagonal matrix $C \in \mathbb{C}^{|\mathcal{E}|\times|\mathcal{E}|}$ such that C_{ii} is the weight of $\varepsilon_i = (h, l) \in \mathcal{E}$ given by Y_{hl}. Then, the *Laplacian* of the undirected graph associated with $\mathbb{G}$ is given by $L = A^\top CA$. Consider the graph $\mathbb{G}$. A *path* $\mathcal{P}(l, h)$, for nodes $l, h \in \mathcal{V}$, is defined as a sequence of nodes $\{n_1, \ldots, n_\ell\}$ such that $n_1 = l$, $n_\ell = h$ and (n_i, n_{i+1}) is an edge of $\mathbb{G}$, for all $i \in \{1, \ldots, \ell - 1\}$.

2. PROBLEM STATEMENT

Consider a microgrid which is connected to the grid at a single point. The microgrid is modeled as an undirected weighted graph $\mathbb{G} = (\mathcal{V}, \mathcal{E}, Y)$, $\mathcal{V} \triangleq \{0, \ldots, N-1\}$, $\mathcal{E} \subseteq \mathcal{V} \times \mathcal{V}$, $Y \in \mathbb{C}^{N\times N}$, where nodes in $\mathcal{V}$ represent buses and edges in $\mathcal{E}$ represent the interconnection lines. Weights are given by the matrix Y and correspond to the line admittances of such interconnection lines. We consider a microgrid with generation and storage capacities. This microgrid has three different types of nodes: i) a single connection point to the grid, represented by node 0, which acts as a slack node, with fixed voltage and unlimited power generation, ii) a subset of nodes $\mathcal{G}$ with generation and storage capacity, and iii) a set $\mathcal{M} = \mathcal{V} \setminus (\{0\} \cup \mathcal{G})$ of nodes with neither generation nor storage capacity. All nodes in $\mathcal{V} \setminus \{0\}$ have a load that must be satisfied.

Let us consider a discrete, finite-time window τ, with T time slots, i.e., $\tau \triangleq \{1, \ldots, T\}$. Each time slot t has an electricity cost $c(t)$ associated with it, which is the price per kWh, given by a map $c : \tau \to \mathbb{R}_{\geq 0}$, and depends on the overall demand satisfied by the utility. The value of $c(t)$ for each $t \in \tau$ is assumed to be known to nodes of the grid, since utility companies make it publicly available. Similarly, for each time slot $t \in \tau$ there is an amount of active power that each generator can provide during the whole time slot t, called $p_{\text{in},l}(t) > 0$, for each $l \in \mathcal{G}$. We assume that this value cannot be controlled, as it is the case with renewable generation, but we can estimate it using forecasting techniques. In order to make the problem slightly more general, the load at each node may also depend on the time

Prepared using rncauth.cls
DOI: 10.1002/rnc

slot $t \in \tau$. For each $l \in \mathcal{V} \setminus \{0\}$, let $p_{\text{load},l}(t) + jq_{\text{load},l}(t)$, $p_{\text{load},l}(t) \geq 0$, be power that must be supplied to a load placed at the node, for all $t \in \tau$.

The problem we would like to solve consists in finding the optimal policy for the reactive power injection, and for the storage charging/discharging rates, that optimizes the microgrid operation defined by the combined objective of minimizing active power generation cost and distribution losses. Before stating the problem more formally, we next describe the model we use to represent a microgrid and the elements involved in it.

2.1. Mathematical model of a microgrid

Let $u_l(t) \in \mathbb{C}$ be the voltage at node $l \in \mathcal{V}$, at time $t \in \tau$. Let $\iota_l(t) \in \mathbb{C}$ be the current flowing through node $l \in \mathcal{V}$. Let A be the incidence matrix associated with $\mathbb{G}$, based on some given ordering on $\mathcal{E}$. For node 0, let $u_0(t)$ be fixed for all $t \in \tau$ and described as $u_0(t) = U_0 e^{j\phi}$. Let $s_l(t) = u_l(t)\hat{\iota}_l(t)$ be the complex apparent power drawn or supplied to node l at time t. Recall that $s_l(t) = P_l(t) + jQ_l(t)$, where $P_l(t)$, $Q_l(t)$ are the active and reactive power at node $l \in \mathcal{V}$, at time $t \in \tau$.

Next, we introduce some compact-form notation. Define $u(t) \triangleq [u_0, u_G^\top(t), u_L^\top(t)]^\top \in \mathbb{C}^{N\times N}$ as the voltage vector for all nodes in the set $\mathcal{V}$, at time $t \in \tau$, where $u_G(t)$ is the vector of all voltages at nodes in $\mathcal{G}$, and $u_L(t)$ is the vector of all voltages in the set $\mathcal{M}$. Likewise, $\iota(t) \triangleq [\iota_0(t), \iota_G^\top(t), \iota_L^\top(t)]^\top$, $s(t) \triangleq [s_0(t), s_G^\top(t) s_L^\top(t)]^\top$, with $s(t) = P(t) + jQ(t)$, $P(t) \triangleq [P_0(t), P_G^\top(t), P_L^\top(t)]^\top$, and $Q(t) \triangleq [q_0(t), Q_G^\top(t), Q_L^\top(t)]^\top$.

The convention for the active power sign is that if $P_l(t) < 0$, power is injected to the l^{th} node, while $P_l(t) > 0$ means that power is drawn from the l^{th} node, for all $l \in \mathcal{V}$, $t \in \tau$. As an example, for a node with load only, it must hold that $P_l(t) \leq 0$ for all $t \in \tau$. Likewise, for a node l with only generation, but neither storage nor load, $P_l(t) \geq 0$ for all $t \in \tau$. Given the type of nodes we consider in the microgrid, we have that $P_G(t) = p_{\text{in},G}(t) - p_{\text{load},G}(t) - v(t)$, where $v(t)$ is a vector whose l^{th} component $v_l(t)$ is the amount of power that is being supplied to the battery at such node, $l \in \{1, \ldots, |\mathcal{G}|\}$. Similarly, $P_L(t) = -p_{\text{load},L}(t)$, for

Prepared using rncauth.cls
DOI: 10.1002/rnc

all $t \in \tau$. Finally, we have that $Q_G(t) = q_{\text{in},G}(t) - q_{\text{load},G}(t)$ and $Q_L(t) = -q_{\text{load},L}(t)$, for all $t \in \tau$. The vector $q_{\text{in},G}(t) \in \mathbb{R}^{|\mathcal{G}|}$ represents the reactive power that is supplied by each generator in $\mathcal{G}$ at time $t \in \tau$.

Then, using the Kirchoff's current and voltage laws, the relation between voltage and current is given by:

$$\begin{aligned} A^\top \mathcal{I}(t) + \iota(t) &= 0 \\ Au(t) + Z\mathcal{I}(t) &= 0, \end{aligned} \tag{1}$$

where $\mathcal{I}(t) \in \mathbb{C}^{|\mathcal{E}|}$ is a vector with the values of current at each edge in $\mathcal{E}$ and time $t \in \tau$, and Z is the diagonal matrix in $\mathbb{C}^{|\mathcal{E}|\times|\mathcal{E}|}$ whose elements are the line impedances in the microgrid.

In the following, we will make the following assumptions on the microgrid parameters. These assumptions have already been used in [10, 11] and are accurate for actual operation conditions in real microgrids.

***Assumption** 2.1* (Large input voltage at the microgrid)
The value of U_0 is very large as compared to the currents provided by the inverters and batteries, or supplied to the loads.

***Assumption** 2.2* (Transmission lines' reactance/resistance ratio)
The microgrid has transmission lines with the same reactance/resistance ratio. Therefore, for all edges $\ell \in \mathcal{E}$, the impedance z_ℓ can be written as $z_\ell = |z_\ell|e^{j\theta}$.

2.2. Mathematical model of a battery

We model a battery with the following dynamics:

$$x_l(t) = x_l(t-1) + \frac{1}{\beta_l} v_l(t), \qquad \forall l \in \mathcal{G}, \quad \forall t \in \tau, \tag{2}$$

Prepared using rncauth.cls
DOI: 10.1002/rnc

where $x_l(t) \in [0,1]$ is the battery state, β_l corresponds to the battery capacity, divided by the length of the time slot. Recall that $v_l(t)$ denotes the power injected to or drained from the battery during the time slot $t \in \tau$. Clearly, the battery has physical constraints, formulated as $v_l \in [V^l_{\rm dis}, V^l_{\rm ch}]$, where $V^l_{\rm dis} < 0$, $-V^l_{\rm dis}$ is the maximum amount of power the battery can discharge during a time slot $t \in \tau$, and $V^l_{\rm ch} > 0$ is the maximum amount the battery can charge. Note that this model assumes that the charger efficiency is one. Assume that the initial state for the battery at node $l \in \mathcal{G}$ is $x_l(0)$. Then, for each $t \in \tau$, the battery charge is given by:

$$x_l(t) = x_l(0) + \frac{1}{\beta_l} \sum_{\ell=1}^{t} v_l(\ell), \qquad \forall l \in \mathcal{G}, \quad \forall t \in \tau.$$

In compact form, denote by $v(t)$ the vector of battery charge/discharge rates at time t, for all nodes in the set $\mathcal{G}$.

2.3. Communication network

Generators and storage systems will coordinate operations by means of a communication network. The communication topology is based on the microgrid topology and the location of the generation/storage nodes in the microgrid.

***Definition** 2.1* (Communication network)

The *communication network* is given by the undirected graph $\mathbb{G}_G = (\mathcal{G} \cup \{0\}, \mathcal{E}_G)$, where $\mathcal{E}_G \subseteq \mathcal{G} \cup \{0\} \times \mathcal{G} \cup \{0\}$ is defined as $\mathcal{E}_G \triangleq \{(l,h) \in \mathcal{G} \cup \{0\} \times \mathcal{G} \cup \{0\} \mid \mathcal{P}(h,l) \cap (\mathcal{G} \cup \{0\}) = \{h,l\}\}$. The set of *neighbors* $\mathcal{N}_G(l)$ of $l \in \mathcal{G} \cup \{0\}$ in the *communication network* is given by $\mathcal{N}_G(l) \triangleq \{h \in \mathcal{G} \cup \{0\} \mid (l,h) \in \mathcal{E}_G\}$.

2.4. The MICROGRID CONTROL PROBLEM

Based on the microgrid and battery models we have presented above, actuation over the microgrid will be established through the decision variables $q_{{\rm in},l}(t)$, which represents the

Prepared using rncauth.cls
DOI: 10.1002/rnc

reactive power supplied by generation systems, and $v_l(t)$, which represents the active power provided by the batteries, for all $l \in \mathcal{G}$, while the input voltage u_0, the energy cost $c(t)$, the loads $p_{\text{load},l}(t)$ and $q_{\text{load},l}(t)$ for $l \in \mathcal{V} \setminus \{0\}$, and the forecasted active power generation $p_{\text{in},l}(t)$, for $l \in \mathcal{G}$, are parameters of the problem, for all $t \in \tau$.

Our objective is to compute optimal reactive power generation and storage control profiles for the time horizon τ. This must be done in such a way that the voltage at each node in $\mathcal{G}$ is maintained within a desirable range and the storage control respects all physical constraints related to the batteries, while a cost is minimized. The cost we consider encompasses two possibly conflicting objectives: i) minimize the cost of active power from the grid and ii) minimize the transmission losses in the transmission lines present in the microgrid. Minimizing transmission losses is a significant objective in Optimal Power Flow and it has been considered in several works [3, 7, 10, 11]. Thus, the cost function is given by:

$$J(u) = \sum_{t \in \tau} (J_{\text{loss}}(u(t)) + \delta J_{\text{power}}(u(t))),$$

where $J_{\text{loss}}(u(t))$ represents the loss in the transmission lines of the microgrid at time slot t, and $J_{\text{power}}(u(t))$ is the overall cost of the active power provided by the utility at time slot t. The trade-off between these possibly conflicting objectives is parameterized by the nonnegative constant $\delta > 0$, which is used to modify the relative importance of $J_{\text{power}}(u(t))$ with respect to $J_{\text{loss}}(u(t))$ in the optimization. The loss in the transmission lines can be expressed as $J_{\text{loss}}(u(t)) = \hat{u}^\top(t) L u(t)$, where $L = A^\top Z_{\text{mag}}^{-1} A$, $Z_{\text{mag}} = \|Z\|_{\mathbb{C}}$ [11], and the power cost is given by $J_{\text{power}}(u(t)) = -c(t)\,\text{Re}(s_0(t)) = -c(t)\,\text{Re}(\hat{\iota}_0(t) u_0(t))$. The negative sign follows the introduced convention for the active power sign. Since $\iota(t)$ can be approximated by Assumption 2.2 on the common transmission lines' reactance/resistance ratio as $\iota(t) = e^{-j\theta} L u(t)$, then $J_{\text{power}}(u(t)) = -\,\text{Re}\{e^{j\theta} \hat{u}^\top(t) L \mathbf{e}_0 \mathbf{e}_0^\top u(t)\} c(t)$.

The following results give us a convenient way of approaching the problem, by writing $u(t)$ as a linear function of the decision variables.

Prepared using rncauth.cls
DOI: 10.1002/rnc

***Lemma** 2.1* (Existence of matrix X [10])

There exists a unique symmetric, positive semidefinite matrix $X \in \mathbb{R}^{N\times N}$, which can be written as:

$$X = \begin{bmatrix} 0 & 0 & 0 \\ 0 & W & F \\ 0 & F^\top & R \end{bmatrix},$$

such that $XL = I_N - \mathbf{1}(\mathbf{e}_0)^\top$ and $X\mathbf{e}_0 = 0$, where $W \in \mathbb{R}^{|\mathcal{G}|\times|\mathcal{G}|}$, $R \in \mathbb{R}^{|\mathcal{M}|\times|\mathcal{M}|}$, and $F \in \mathbb{R}^{|\mathcal{G}|\times|\mathcal{M}|}$.

The physical meaning of the matrix X is widely discussed in [10], [11]. One of the properties of X is that the product $(\mathbf{e}_h - \mathbf{e}_l)^\top X(\mathbf{e}_h - \mathbf{e}_l)$ corresponds to the effective impedance from node $h \in \mathcal{V}$ to node $l \in \mathcal{V}$. The following result follows directly from Lemmas 3 and 4 in [11].

***Lemma** 2.2* (Matrix G)

There exists a unique symmetric matrix G, such that:

$$\begin{bmatrix} 0 & 0 \\ 0 & W \end{bmatrix} \mathsf{G} = I_{|\mathcal{G}|+1} - \mathbf{1}(\mathbf{e}_0)^\top, \qquad\qquad \mathsf{G}\mathbf{1} = 0.$$

Moreover, the matrix G has a sparsity induced by the communication network graph, this is, $\mathsf{G}_{ij} \neq 0$ if and only if $j \in \mathcal{N}_G(i)$. The matrix W is a block of the matrix X described in Lemma 2.1.

From the result above, it is immediately noted that the matrix W is invertible. We can also see that its inverse matrix corresponds to a block in the matrix G, which means that it also has a sparsity induced by the communication network graph.

The following result provides a linearization of the relation between voltages and powers on the microgrid.

Prepared using rncauth.cls
DOI: 10.1002/rnc

***Lemma** 2.3* (Microgrid voltage approximation [11])
Consider (1), along with $s_l(t) = u_l(t)\hat{\imath}_l(t)$. Then, the microgrid voltages satisfy:

$$\begin{bmatrix} u_0(t) \\ u_G(t) \\ u_L(t) \end{bmatrix} = e^{j\phi} \left(U_0 \mathbf{1} + \frac{e^{j\theta}}{U_0} \begin{bmatrix} 0 & 0 & 0 \\ 0 & W & F \\ 0 & F^\top & R \end{bmatrix} \begin{bmatrix} 0 \\ \hat{s}_G(t)) \\ \hat{s}_L(t) \end{bmatrix} \right) + o\left(\frac{1}{U_0}\right). \tag{3}$$

Notice that by Assumption 2.1 on the large magnitude of the input voltage, the relaxation given by Lemma 2.3 provides an accurate approximation, as the term $o\left(\frac{1}{U_0}\right)$ vanishes for large values of U_0.

Having established some relaxations on the nonlinear equations describing the microgrid physics, we describe the MICROGRID CONTROL PROBLEM as follows:

$$\begin{aligned} &\min_{q_{\text{in},G},v} \sum_{t\in\tau} (J_{\text{loss}}(u(t)) + \delta J_{\text{power}}(u(t))) \\ &\text{s.t.} \begin{cases} U_{\min} \le \|u_l(t)\|_{\mathbb{C}} \le U_{\max}, & l \in \mathcal{G}, t \in \tau \\ V_{\text{dis}}^l \le v_l(t) \le V_{\text{ch}}^l, & l \in \mathcal{G}, t \in \tau \\ 0 \le x_l(0) + \frac{1}{\beta_l} \sum_{s=1}^{T} v_l(s) \le 1, & l \in \mathcal{G}, t \in \tau \\ \text{Equation (3) holds.} \end{cases} \end{aligned} \tag{4}$$

Clearly, the lower bound constraint on the voltage magnitude introduces a non-convex constraint to the problem. In order to follow the convexification idea in [11], we define $w_G(t)$, as a vector in $\mathbb{R}^{|\mathcal{G}|}$, whose components are the squares of the magnitudes of the complex voltages $u_l(t)$, normalized by U_0^2, i.e., $w_l(t) \triangleq \|u_l(t)\|_{\mathbb{C}}^2 U_0^{-2}$, for $l \in \mathcal{G}$. After some manipulation, from (3), we obtain:

$$w_G(t) = \mathbf{1} + \frac{2}{U_0^2} \left(\cos\theta \Big(W P_G(t) + F P_L(t) \Big) \quad + \sin\theta \Big(W Q_G(t) + F Q_L(t) \Big) \right) + o\left(\frac{1}{U_0^2}\right). \tag{5}$$

Prepared using rncauth.cls
DOI: 10.1002/rnc

Thus, we can write the constraints on the voltage magnitude as:

$$W_{\min} = \frac{U_{\min}^2}{U_0^2} \leq w_l(t) \leq \frac{U_{\max}^2}{U_0^2} = W_{\max},$$

for all $l \in \mathcal{G}$, $t \in \tau$. Clearly, as $U_{\min}$, $U_{\max}$ have in practice a similar order-of-magnitude than that of U_0, it holds that $U_0^{-2}U_{\min}^2$, $U_0^{-2}U_{\max}^2$ are close to one. For large values of U_0, (5) is affine in the decision variables $q_{\text{in},G}(t)$, $v(t)$, hence the constraint above is convex.

3. DISTRIBUTED REACTIVE POWER AND STORAGE CONTROL ALGORITHM

In order to solve the MICROGRID CONTROL PROBLEM in a distributed way, we propose an extension of the dual decomposition approach presented in [11]. Here we optimize not only the reactive power injection, but also on the battery charge/discharge, considering the physical constraints of the battery control. The fact that we also consider a different cost function modifies the algorithm dynamics. The dual decomposition algorithm consists of performing a gradient ascent on the Lagrangian with respect to the dual variables of the problem, while an unconstrained optimization with respect to the primal variables, parameterized by the estimated dual variables is executed.

The Lagrangian for the optimization problem is given by:

$$\begin{aligned}
\mathcal{L}(q_{\text{in},G},v,\psi) = J(q_G, v) &+ \sum_{t=1}^{T} \underline{\lambda}^\top(t)(W_{\min} - w_G(t)) + \sum_{t=1}^{T} \overline{\lambda}^\top(t)(w_G(t) - W_{\max}) \\
&+ \sum_{t=1}^{T} \underline{\eta}^\top(t)\mathbf{d}(\Delta V)^{-1}(V_{\text{dis}} - v(t)) + \sum_{t=1}^{T} \overline{\eta}^\top(t)\mathbf{d}(\Delta V)^{-1}(v(t) - V_{\text{ch}}) \\
&- \sum_{t=1}^{T} \underline{\mu}^\top(t) \left(x(0) + \mathbf{d}(\beta^{-1}) \sum_{h=1}^{t} v(h) \right) \\
&+ \sum_{t=1}^{T} \overline{\mu}^\top(t) \left(x(0) + \mathbf{d}(\beta^{-1}) \sum_{h=1}^{t} v(h) - 1 \right),
\end{aligned}$$

Prepared using rncauth.cls
DOI: 10.1002/rnc

where $\underline{\lambda}(t), \overline{\lambda}(t), \underline{\eta}(t), \overline{\eta}(t), \underline{\mu}(t), \overline{\mu}(t) \succeq 0$, for all $t \in \tau$, are Lagrange multipliers, and $\mathbf{d}(\beta^{-1}) \in \mathbb{R}^{|\mathcal{G}|\times|\mathcal{G}|}$ is a diagonal matrix such that $\mathbf{d}(\beta^{-1})_{ll} = \frac{1}{\beta_l}$, for all $l \in \{1, \ldots, |\mathcal{G}|\}$. We introduce $\mathbf{d}(\Delta V) \in \mathbb{R}^{|\mathcal{G}|\times|\mathcal{G}|}$ as a diagonal matrix that works as a regularization parameter, such that $\mathbf{d}(\Delta V)_{ll} \triangleq V^l_{\text{ch}} - V^l_{\text{dis}}$, for all $l \in \{1, \ldots, |\mathcal{G}|\}$.

Let us define as a compact representation of the dual variables: $\underline{\lambda} \triangleq [\underline{\lambda}^\top(1), \ldots, \underline{\lambda}^\top(T)]^\top \in \mathbb{R}^{|\mathcal{G}|T}_{\geq 0}$, $\underline{\eta} \triangleq [\underline{\eta}^\top(1), \ldots, \underline{\eta}^\top(T)]^\top \in \mathbb{R}^{|\mathcal{G}|T}_{\geq 0}$, $\underline{\mu} \triangleq [\underline{\mu}^\top(1), \ldots, \underline{\mu}^\top(T)]^\top \in \mathbb{R}^{|\mathcal{G}|T}_{\geq 0}$, (resp. $\overline{\lambda}$, $\overline{\eta}$, $\overline{\mu}$), $\psi(t) \triangleq [\overline{\lambda}^\top(t), \underline{\lambda}^\top(t), \overline{\eta}^\top(t), \underline{\eta}^\top(t), \overline{\mu}^\top(t), \underline{\mu}^\top(t)]^\top$, and a variable $\psi \triangleq [\overline{\lambda}^\top, \underline{\lambda}^\top, \overline{\eta}^\top, \underline{\eta}^\top, \overline{\mu}^\top, \underline{\mu}^\top]^\top \in \mathbb{R}^r_{\geq 0}$, where $r \triangleq 6T|\mathcal{G}|$. The dual decomposition algorithm is given by:

$$(q^k_{\text{in},G}, v^k) = \text{argmin}_{q_{\text{in},G}, v}(\mathcal{L}(q_{\text{in},G}, v, \psi^k)), \tag{6}$$

$$\psi^{k+1} = \left[\psi^k + \gamma \nabla_\psi \mathcal{L}(q^k_{\text{in},G}, v^k, \psi^k)\right]_+, \tag{7}$$

where $\nabla_\psi \mathcal{L}$ is the gradient of $\mathcal{L}$ with respect to the dual variable ψ, and $[\cdot]_+$ is the projection operator onto the positive orthant. The parameter γ is a small enough positive scalar to be characterized later.

Since the Lagrangian is a quadratic function of $(q_{\text{in},G}, v)$, a minimizer for $\mathcal{L}(q_{\text{in},G}, v, \psi^k)$ can be found directly by solving $\nabla_{q_{\text{in},G}, v}\mathcal{L}(q_{\text{in},G}, v, \psi^k) = 0$. Some algebraic manipulations lead to:

$$q^k_{\text{in},G}(t) = q_{\text{load},G}(t) + W^{-1}F q_{\text{load},L}(t) - \sin\theta[\overline{\lambda}^k(t) - \underline{\lambda}^k(t)] \tag{8}$$

$$\begin{aligned} v^k(t) = &- p_{\text{load},G}(t) - p_{\text{in},G}(t) - W^{-1}F p_{\text{load},L}(t) + \cos\theta[\overline{\lambda}^k(t) - \underline{\lambda}^k(t)] \\ &- \frac{U_0^2}{2} W^{-1}\left(\mathbf{d}(\Delta V)^{-1}(\overline{\eta}^k(t) - \underline{\eta}^k(t)) + \sum_{h=t}^{T} \mathbf{d}(\beta^{-1})(\overline{\mu}^k(h) - \underline{\mu}^k(h)) + \delta c(t)\mathbf{1}\right), \end{aligned} \tag{9}$$

Prepared using rncauth.cls
DOI: 10.1002/rnc

for all $t \in \tau$. Formulas (8), (9) are obtained as follows. First, the derivative of $\mathcal{L}$ is computed with respect to the variables $q_{\text{in},G}(t)$ and $v(t)$, for all t. To this end, a chain rule is used by which $\mathcal{L}$ is differentiated with respect to $u(t)$ and $w_G(t)$, and in turn, $u(t)$ and $w_G(t)$ are differentiated with respect to $q_{\text{in},(}(t)$ and $v(t)$. Next, terms of $o\left(\frac{1}{U_0^2}\right)$ are neglected. The remaining linear equations are set equal to zero and a solution in $q_{\text{in},G}(t)$ and $v(t)$, for all $t \in \tau$, is found. This leads to expressions (8), (9).

Since the Lagrangian is linear in the dual variables, the derivative with respect to each of them is merely the expression representing the constraint associated with that dual variable. Thus, the gradient ascent algorithm for the dual variables becomes:

$$
\begin{aligned}
\overline{\lambda}^{k+1}(t) &= \left[\overline{\lambda}^{k}(t) + \gamma(w_G^k(t) - W_{\max})\right]_+, \\
\underline{\lambda}^{k+1}(t) &= \left[\underline{\lambda}^{k}(t) + \gamma(W_{\min} - w_G^k(t))\right]_+, \\
\overline{\eta}^{k+1}(t) &= \left[\overline{\eta}^{k}(t) + \gamma \mathbf{d}(\Delta V)^{-1}(v^k(t) - V_{\text{ch}})\right]_+, \\
\underline{\eta}^{k+1}(t) &= \left[\underline{\eta}^{k}(t) + \gamma \mathbf{d}(\Delta V)^{-1}(V_{\text{dis}} - v^k(t))\right]_+, \\
\overline{\mu}^{k+1}(t) &= \left[\overline{\mu}^{k}(t) + \gamma\left(x(0) + \sum_{h=1}^{t} \mathbf{d}(\beta^{-1})v^k(h) - \mathbf{1}\right)\right]_+, \\
\underline{\mu}^{k+1}(t) &= \left[\underline{\mu}^{k}(t) - \gamma\left(x(0) + \sum_{h=1}^{t} \mathbf{d}(\beta^{-1})v^k(h)\right)\right]_+,
\end{aligned}
\tag{10}
$$

for all $t \in \tau$, with a common parameter γ. Following similar computations as in [11], one can obtain the following result:

***Lemma** 3.1* (Distributed algorithm)

The expressions in (8), (9) can be approximated by:

$$
\begin{aligned}
q_{\text{in},G}^k(t) = \text{Im}\left(e^{-j\theta}\begin{bmatrix} 0 & \mathbf{d}(\overline{u}_G^{k-1}(t)) \end{bmatrix} \mathsf{G} \begin{bmatrix} u_0^{k-1}(t) \\ u_G^{k-1}(t) \end{bmatrix}\right) + q_{\text{in},G}^{k-1}(t) + o\left(\frac{1}{U_0^2}\right) \\
- \sin\theta[\overline{\lambda}^k(t) - \underline{\lambda}^k(t)],
\end{aligned}
\tag{11}
$$

Prepared using rncauth.cls
DOI: 10.1002/rnc

$$v^k(t) = \mathrm{Re}\left(e^{-j\theta} \begin{bmatrix} 0 & \mathbf{d}(\overline{u}_G^{k-1}(t)) \end{bmatrix} \mathsf{G} \begin{bmatrix} u_0^{k-1}(t) \\ u_G^{k-1}(t) \end{bmatrix} \right) + v^{k-1}(t) + \cos\theta(\overline{\lambda}^k(t) - \underline{\lambda}^k(t)) \tag{12}$$

$$- \frac{U_0^2}{2} W^{-1} \left(\mathbf{d}(\Delta V)^{-1}(\overline{\eta}^k(t) - \underline{\eta}^k(t)) + \sum_{h=t}^{T} \mathbf{d}(\beta^{-1})(\overline{\mu}^k(h) - \underline{\mu}^k(h)) + \delta c(t)\mathbf{1} \right),$$

$$+ o\left(\frac{1}{U_0^2}\right), \tag{13}$$

for all $t \in \tau$.

The result above provides an update rule that can be executed by each of the nodes where some type of decision can be made, which in turn is distributed according to the sparsity of G. The proposed updating rule described by (10),(11) and (12) is referred to as MICROGRID CONTROL ALGORITHM and is summarized in Algorithm 1.

The following result establishes that the MICROGRID CONTROL ALGORITHM converges asymptotically to the optimal solution of the problem defined in (4), provided the parameter γ is small enough.

***Theorem** 3.1* (Algorithm convergence)

Let assumptions 2.1, 2.2 on the input voltage magnitude and the transmission lines' impedance angle hold. Assume that the MICROGRID CONTROL PROBLEM in (4) is feasible. Then, for $\gamma < \frac{2}{\rho(M)}$, where M is described in Definition A.3, the execution of the MICROGRID CONTROL ALGORITHM (Algorithm 1) by each node $l \in \mathcal{G}$, leads to $q_{\mathrm{in},G}^k(t) \to q_{\mathrm{in},G}^\star(t)$, $v^k(t) \to v^\star(t)$, for all $t \in \tau$, where $(q_{\mathrm{in},G}^\star,\ v^\star)$ is the unique optimizer of the MICROGRID CONTROL PROBLEM.

The proof of this result can be found in Appendix B.

Prepared using rncauth.cls
DOI: 10.1002/rnc

Algorithm 1: The MICROGRID CONTROL ALGORITHM. Execution for node $l \in \mathcal{G}$

Input: $w_l^{k-1}(t)$, $\overline{\eta}_l^{k-1}(t)$, $\underline{\eta}_l^{k-1}(t)$, $\overline{\mu}_l^{k-1}(t)$, $\underline{\mu}_l^{k-1}(t)$, $q_l^{k-1}(t)$, $v_l^{k-1}(t)$ (also $\overline{\lambda}_l^{k-1}(t)$, $\underline{\lambda}_l^{k-1}(t)$, if $l \in \mathcal{G}$), for all $t \in \tau$

for $t \in \{1, \ldots, T\}$ **do**

$\overline{\lambda}_l^k(t) = \left[\overline{\lambda}_l^{k-1}(t) + \gamma(w_l^{k-1}(t) - W_{\max})\right]_+$

$\underline{\lambda}_l^k(t) = \left[\underline{\lambda}_l^{k-1}(t) + \gamma(W_{\min} - w_l^{k-1}(t))\right]_+$

$\overline{\eta}_l^k(t) = \left[\overline{\eta}_l^{k-1}(t) + \gamma\frac{1}{\Delta V_l}(v_l^{k-1}(t) - V_{\text{ch}}^l)\right]_+$

$\underline{\eta}_l^k(t) = \left[\underline{\eta}_l^{k-1}(t) + \gamma\frac{1}{\Delta V_l}(V_{\text{dis}}^l - v_l^{k-1}(t))\right]_+$

$\overline{\mu}_l^k(t) = \left[\overline{\mu}_l^{k-1}(t) + \gamma\left(x_l(0) + \frac{\alpha_l}{\beta_l}\sum_{h=1}^t v_l^{k-1}(h) - 1\right)\right]_+$

$\underline{\mu}_l^k(t) = \left[\underline{\mu}_l^{k-1}(t) + \gamma\left(-x_l(0) - \frac{\alpha_l}{\beta_l}\sum_{h=1}^t v_l^{k-1}(h)\right)\right]_+$

end

Gather $\overline{\eta}_h^k(t)$, $\underline{\eta}_h^k(t)$, $\overline{\mu}_h^k(t)$, $\underline{\mu}_h^k(t)$, for all $t \in \tau$, for all $h \in \mathcal{N}_S(l) \setminus \{0\}$

Gather $u_h^{k-1}(t)$ for all $t \in \tau$, for all $h \in \mathcal{N}_S(l)$ (for all $h \in \mathcal{N}_S(l) \cup \mathcal{N}_G(l)$ if $l \in \mathcal{G}$)

for $t \in \{1, \ldots, T\}$ **do**

$v_l^k(t) = v_l^{k-1}(t) + \cos\theta(\overline{\lambda}_l^k(t) - \underline{\lambda}_l^k(t)) + \sum_{h\in\mathcal{N}_G(l)} \mathsf{G}_{lh}\Big(\|u_l^{k-1}(t)\|_{\mathbb{C}}\|u_h^{k-1}(t)\|_{\mathbb{C}}$ $\cos(\angle u_h^{k-1}(t) - \angle u_l^{k-1}(t) - \theta)\Big) + \frac{U_0^2}{2}\sum_{h\in\mathcal{N}_G(l)\setminus\{0\}} \mathsf{G}_{lh}\Big(-\frac{1}{\Delta V_l}(\overline{\eta}_h^k(t) - \underline{\eta}_h^k(t)) -$ $\frac{1}{\beta_h}\sum_{b=t}^T(\overline{\mu}_h^k(b) - \underline{\mu}_h^k(b)) - \delta c(t)\Big)$

$q_{\text{in},l}^k(t) = q_{\text{in},l}^{k-1} - \sin\theta(\overline{\lambda}_l^k(t) - \underline{\lambda}_l^k(t)) + \sum_{h\in\mathcal{N}_G(l)} \mathsf{G}_{lh}\Big(\|u_l^{k-1}(t)\|_{\mathbb{C}}\|u_h^{k-1}(t)\|_{\mathbb{C}}$ $\sin(\angle u_h^{k-1}(t) - \angle u_l^{k-1}(t) - \theta)\Big)$

end

4. VOLTAGE PREDICTION

In order to compute $q_{\text{in},G}(t), v(t)$, for $t \in \tau$, the MICROGRID CONTROL ALGORITHM requires voltage information for all $t \in \tau$. However, this information is not available for two reasons: i) voltages $u(t)$ depend on the power injections at all the nodes of the microgrid at time $t \in \tau$, i.e., they depend on future values of the decision variables, and ii) although for time $t = 1$, it is theoretically possible to inject the power given by decision variables $v^k(1)$ and $q_{\text{in},G}^k(1)$ into the system, these variables are only asymptotically feasible. Then, it may be either harmful or impossible to inject such power values into the actual microgrid. Thus, it is necessary to use a model to predict values of $u(t)$, for $t \in \tau$. Recall that a microgrid is modeled by the nonlinear memoryless system of equations formulated in (1). Finding the solution for voltages $u(t)$ given $P(t)$, $Q(t)$ and u_0 is not only a computationally expensive

Prepared using rncauth.cls
DOI: 10.1002/rnc

procedure, but it is also not distributed. We formulate two alternatives to address this problem.

4.1. A multilayer control approach

A first possibility is to define an additional layer for the control, which contains a model of the microgrid, and is such that it can exchange information with all nodes in $\mathcal{G}$. Thus, the control structure has two layers: the upper layer with a 'super agent' that knows the microgrid model, and the lower layer, with the node controllers. At each iteration, nodes in $\mathcal{G}$ will provide the super agent in the upper layer the value of $q^k_{\text{in},G}$ and v^k. The agent uses these values to compute u^k by solving the power flow equations in (1). Then, the agent provides the node controllers with u^k according to their sparsity in the sense of the network topology of Definition 2.1. Then, the dual decomposition algorithm is executed again. By means of this approach, part of the computations are carried out in a centralized way. Even though part of the computations are parallelized, i.e., the control computations, the centralized computations performed by the super agent destroy the scalability and robustness properties that justify the use of a distributed algorithm.

4.2. Distributed approximation

An alternative is the VOLTAGE PREDICTION ALGORITHM: a novel idea which is based on the voltage expression given in (3). It consists of executing several sub-iterations at each iteration k of the control computation, in order to approximate the voltage u^k for the computation of $q^{k+1}_{\text{in},G}$ and v^{k+1}. Figure 1 shows the interaction between the MICROGRID CONTROL ALGORITHM and the VOLTAGE PREDICTION ALGORITHM. Let us assume that all the loads in nodes that belong to $\mathcal{M}$ are constant, for all $t \in \tau$, i.e., $s_L(t) = s_L$, for all $t \in \tau$. Let us consider $u_0 \triangleq [U_0 e^{j\phi}, u_{0,G}^\top, u_{0,L}^\top]^\top \in \mathbb{R}^N$ and $s_0 \triangleq [S_0, s_{0,G}^\top, s_L^\top]^\top \in \mathbb{R}^N$, with $s_{0,L} = p_L + jq_L$, such that the pair u_0, s_0 solves the power flow equations that model the microgrid. Assume that each node $l \in \mathcal{G}$ knows $u_{0,l}$ and $s_{0,l}$, where $u_{0,l}$ and $s_{0,l}$

Prepared using rncauth.cls
DOI: 10.1002/rnc

denote the l^{th} components of u_0 and s_0 respectively, which means that the node l requires entirely local information.

Using the expression in (3), we have that:

$$\Delta u_t = e^{j\phi}\left(\frac{e^{j\theta}}{U_0} W \Delta \hat{s}_t\right),$$

where $\Delta u_t \triangleq u_G(t) - u_{G,0}$, and $\Delta \hat{s}_t \triangleq \hat{s}_G(t) - \hat{s}_{G,0}$, for all $t \in \{1, \ldots, T\}$. Then, we obtain:

$$\begin{aligned}
\mathrm{Re}(\Delta u_t) &= W\left(\frac{\cos(\theta+\phi)}{U_0}\,\mathrm{Re}(\Delta \hat{s}_t) - \frac{\sin(\theta+\phi)}{U_0}\,\mathrm{Im}(\Delta \hat{s}_t)\right),\\
\mathrm{Im}(\Delta u_t) &= W\left(\frac{\sin(\theta+\phi)}{U_0}\,\mathrm{Re}(\Delta \hat{s}_t) + \frac{\cos(\theta+\phi)}{U_0}\,\mathrm{Im}(\Delta \hat{s}_t)\right).
\end{aligned}$$

Notice that the l^{th} component of $\Delta \hat{s}_t$ is known to node $l \in \mathcal{G}$ for all $t \in \tau$. Since W is invertible, it is possible to solve Δu_t, using the Jacobi overrelaxation algorithm, as follows:

$$u_{e,t}^{\ell+1} = (1-h)u_{e,t}^{\ell} - h\mathbf{d}(W^e)^{-1}\left((W^e - \mathbf{d}(W^e))u_{e,t}^{\ell} - s_{e,t}^{\ell}\right), \tag{14}$$

where $W^e \triangleq I_2 \otimes W^{-1}$ and:

$$\begin{aligned}
u_{e,t} &= \begin{bmatrix} \mathrm{Re}(\Delta u_t) \\ \\ \mathrm{Im}(\Delta u_t) \end{bmatrix},\\
s_{e,t} &= \begin{bmatrix} \frac{\cos(\theta+\phi)}{U_0}\,\mathrm{Re}(\Delta \hat{s}_t) - \frac{\sin(\theta+\phi)}{U_0}\,\mathrm{Im}(\Delta \hat{s}_t) \\ \frac{\sin(\theta+\phi)}{U_0}\,\mathrm{Re}(\Delta \hat{s}_t) + \frac{\cos(\theta+\phi)}{U_0}\,\mathrm{Im}(\Delta \hat{s}_t) \end{bmatrix}.
\end{aligned}$$

By construction of W, it also holds that the diagonal elements of W^e are strictly positive. Then the matrix $\mathbf{d}(W^e)^{-1}$ is well defined. Given that W^{-1} is symmetric and positive definite, W^e is also symmetric and positive definite. Then, it holds that if $h < 2/|\mathcal{G}|$, the Jacobi overrelaxation converges from any initial condition and also presents a linear rate

Prepared using rncauth.cls
DOI: 10.1002/rnc

of convergence. Since W^{-1} is distributed in the sense of the communication network in Definition 2.1, the computation of u can be made using only local information. Algorithm 2

Algorithm 2: The VOLTAGE PREDICTION ALGORITHM. Execution for node $l \in \mathcal{G}$

Input: $v_l^k(t)$, $q_{\text{in},l}^k(t)$ (if $l \in \mathcal{G}$), for all $t \in \tau$.

for $t = \{1, \ldots, T\}$ **do**
  $\delta_{t,Re}^0(l) = 0$
  $\delta_{t,Im}^0(l) = 0$
  $s_{l,t} = p_{\text{in},l}(t) - p_{\text{load},l}(t) - v_l^k(t) + j(q_{\text{in},l}^k(t) - q_{\text{load},l}(t))$
  $b_{t,Re} = \frac{\cos(\theta+\phi)}{U_0} \operatorname{Re}(s_{l,t} - s_{l,0}) - \frac{\sin(\theta+\phi)}{U_0} \operatorname{Im}(s_{l,t} - s_{l,0})$
  $b_{t,Im} = \frac{\sin(\theta+\phi)}{U_0} \operatorname{Re}(s_{l,t} - s_{l,0}) + \frac{\cos(\theta+\phi)}{U_0} \operatorname{Im}(s_{l,t} - s_{l,0})$
end
for $\ell \in \{1, \ldots, \ell_{\max} - 1\}$ **do**
  for $t = \{1, \ldots, T\}$ **do**
    $\delta_{t,Re}^{\ell+1}(l) = (1-h)\delta_{t,Re}^{\ell}(l) - \frac{h}{\mathsf{G}_{S,ll}} \left(\sum_{r \in \mathcal{N}_S(l) \setminus \{0,l\}} \mathsf{G}_{S,lr} \delta_{t,Re}^{\ell}(r) - b_{t,Re} \right)$
    $\delta_{t,Im}^{\ell+1}(l) = (1-h)\delta_{t,Im}^{\ell}(l) - \frac{h}{\mathsf{G}_{S,ll}} \left(\sum_{r \in \mathcal{N}_S(l) \setminus \{0,l\}} \mathsf{G}_{S,lr} \delta_{t,Im}^{\ell}(r) - b_{t,Im} \right)$
  end
end
for $t = \{1, \ldots, T\}$ **do**
  $u_l^k(t) \approx \delta_{t,Re}^{\ell_{\max}}(l) + j\delta_{t,Im}^{\ell_{\max}}(l) + u_{l,0}$
end

summarizes the prediction procedure for each node $l \in \mathcal{G}$.

[Figure 1 about here.]

Notice that a fast execution of this algorithm (until some error tolerance is reached) at the end of each iteration of the dual decomposition algorithm can give an approximation of $u_G(t)$, $t \in \tau$, for the next iteration.

Let us recall that the load and the active power generation at all nodes are system parameters that come from forecasting processes. In the particular case of load forecasting, persistence models are widely used. A persistence model assumes that the best forecast for a variable in the near future is the current value of that variable. It leads to an estimate of a future step for loads in nodes $l \in \mathcal{M}$ computed as follows:

$$s_L(t+1) = s_L(t).$$

Prepared using rncauth.cls
DOI: 10.1002/rnc

A propagation of this estimation over the whole time horizon τ leads to a load estimation in which $s_L(t) = s_L$ for all $t \in \tau$, which is the setting under which our distributed prediction model works. Thus, even though the assumption that the load of nodes in $\mathcal{M}$ does not vary with time seems to be restrictive, it is not introducing any additional assumptions than those that are already posed in real applications.

5. SIMULATION RESULTS AND DISCUSSION

We implement the MICROGRID CONTROL ALGORITHM on a single-phase approximation of the IEEE 37 standard model, with the same location of generators as in [11]. In addition, we add 4 nodes that have only storage capacity and no generation. The connection to the grid is made through node 0. The microgrid scheme is shown on Figure 2.

[Figure 2 about here.]

The complete list of the microgrid parameters, as well as the commented simulation code we have used, can be found at `http://fausto.dynamic.ucsd.edu/andres/project_reactive.html`. Simulations have been run by coupling the dual decomposition algorithm with the voltage prediction algorithm, following the structure given in Figure 1. We consider fixed loads for the load nodes, and a 5-step prediction horizon, i.e., $\tau = \{1, \ldots, 5\}$. Moreover, we establish a desirable voltage regulation range of $[0.95, 1.05]$ p.u., this is relative to the voltage of the connection point, established as $4.8kV$. The parameter γ is chosen to be 0.0728, which is $0.8/\|M\|_\infty$, satisfying the condition in Theorem 3.1. We use for the VOLTAGE PREDICTION ALGORITHM a parameter $h = 0.9889$. Note that we take advantage of the knowledge of the microgrid topology to derive a larger parameter which, even though does not satisfy the upper bound $2/|\mathcal{G}|$, allows for a spectral radius of $I - hW^e$ less than one, leading to stability. We truncate the voltage approximation after 100 iterations of the fast scale execution.

[Figure 3 about here.]

Prepared using rncauth.cls
DOI: 10.1002/rnc

[Figure 4 about here.]

[Figure 5 about here.]

Figure 3 shows the evolution of the decision variables for the whole time horizon, for node 4. Dashed lines represent the optimal values for the decision variables (presenting some overlap). It can be seen that the algorithm leads the decision variables to their optimizers.

Notice that there is a remarkable difference between the amount of iterations that it takes the variable $q_{\text{in},G}$ to converge and those for the variable v. There are two main observed reasons for this difference: the first one is that the amount of local constraints related to the variable v is very large as compared to those affecting $q_{\text{in},G}$. The second reason is that the geometry of the feasible set given by the local constraints on v activates some multipliers that in their optimal state should be zero. In particular, we observe a very fast and large growth in the $\underline{\eta}$ multipliers. Once the satisfaction of the $\underline{\mu}$ constraints guarantee the satisfaction of the $\underline{\eta}$ constraints, the components of $\underline{\eta}$ start to decrease. However, the nonlinear dynamics for the multipliers do not allow for a fast decrease rate. It can be seen in Figures 4, 5 that the $\underline{\eta}$, $\underline{\mu}$ multipliers grow very fast, however, the multipliers $\underline{\eta}$ eventually start a very slow decrease to end up reaching the optimal value 0. This slow decrease leads to very large number of iterations for convergence, which may affect the possibility of using the algorithm in applications with short discretization steps. Recall that for each iteration of the controller-predictor loop, the predictor executes 100 iterations, all of them requiring communication between neighboring nodes. This number has been chosen in order to guarantee that the first two significant figures of the approximation reach those of the real value for all voltages. This is not a very conservative number, since a lower accuracy in the approximation may severely affect the optimization result. Since the parameter γ is near the limit for stability, the speed of convergence cannot be significantly improved. We have tested the speed of execution of several iterations of the algorithm in a computer with processor 2.8GHz Intel Core i7, and 8GB 1333 MHz RAM, and on average, each iteration

Prepared using rncauth.cls
DOI: 10.1002/rnc

takes 0.0364 seconds. Of course, the computations for all nodes have been performed in a sequential manner, while they are meant to be performed in a parallel way. Nevertheless, the simulation for 60×10^3 iterations that is shown in the case study required more than 36 minutes to run.

6. CONCLUSIONS AND FUTURE WORK

This work presents a distributed algorithm for the computation of predictive control sequences of reactive power and storage in microgrids. The algorithm uses forecasted parameters such as the electricity cost in time and the solar-power generation, in order to compute the reactive power that must be injected by generators and the charging/charging rate that storage devices must follow in order to minimize electricity cost and also transmission losses. The design is based on a previous convexification approach which relaxes the power flow equations onto a linear relation between power and voltage in a microgrid, under some assumptions on impedances in the transmission lines and the magnitude of the input voltage. New constraints on voltage regulation, and operational constraints on the storage systems are considered. Then, a dual-decomposition-based dynamics is presented and thoroughly analyzed, concluding that the dynamics globally converge to the unique optimizer of the problem. Finally, we present two ways of computing the voltage values that are required in order to obtain future values of the decision variables, i.e., reactive power generation and storage control, including a novel distributed prediction model. Simulations illustrate the algorithm performance.

Future work will focus on designing dynamics with faster convergence, which could be practically implementable for short-time prediction horizons and relatively small discretization steps, in basic computation devices such as Programmable Logic Controllers (PLCs) and Remote Terminal Units (RTUs).

Prepared using rncauth.cls
DOI: 10.1002/rnc

APPENDIX

A. AUXILIARY RESULTS FOR THE PROOF OF THEOREM 3.1

***Lemma** A.1* (Optimizers and fixed points of the algorithm)

The vector $\psi^\star$ is an optimizer of the dual of the MICROGRID CONTROL PROBLEM, and $(q^\star_{\text{in},G}, v^\star)$ is an optimizer of the MICROGRID CONTROL PROBLEM if and only if $(\psi^\star, q^\star_{\text{in},G}, v^\star)$ is a fixed point of the MICROGRID CONTROL ALGORITHM.

Proof

It is easy to show that if $(\psi^\star, q^\star_{\text{in},G}, v^\star)$ is a fixed point of the dynamics in (10), then $(\psi^\star, q^\star_{\text{in},G}, v^\star)$ satisfies the KKT conditions for the MICROGRID CONTROL PROBLEM in (4). Since the cost J is continuously differentiable and the constraints are affine functions, the KKT conditions are sufficient and necessary, hence $(\psi^\star, q^\star_{\text{in},G}, v^\star)$ is an optimizer of the primal-dual problem. Next, let us consider any $(\psi^\star, q^\star_{\text{in},G}, v^\star)$, which is an optimizer of the MICROGRID CONTROL PROBLEM in (4). The KKT conditions must hold at this point. Using the complementary slackness condition onto (10), we can see that if $\psi^k = \psi^\star$, then $\psi^{k+1} = \psi^\star$. Further, it is easy to see from the expressions in (8), (9) that $q^{k+1}_{\text{in},G} = q^k_{\text{in},G} = q^\star_{\text{in},G}$, and $v^{k+1} = v^k = v^\star$, meaning that $(\psi^\star, q^\star_{\text{in},G}, v^\star)$ is a fixed point for the algorithm. □

***Definition** A.1* (Kronecker product [13])

Consider matrices $A \in \mathbb{R}^{m\times n}$, with entries a_{ij}, $B \in \mathbb{R}^{p\times q}$, with entries b_{ij}. The Kronecker product $C = A \otimes B$ returns the block matrix in $\mathbb{R}^{mp\times nq}$ such that the blocks are $(C)_{kl} = a_{kl}B$, for $k \in \{1,\dots,m\}$, $l \in \{1,\dots,n\}$.

***Definition** A.2* (Khatri-Rao product [13])

Consider matrices $A \in \mathbb{R}^{m\times n}$, with entries a_{ij}, $B \in \mathbb{R}^{p\times q}$, with entries b_{ij}. Let A be block partitioned in blocks $(A)_{kl} \in \mathbb{R}^{m_k\times n_l}$, and B in blocks $(B)_{kl} \in \mathbb{R}^{p_k\times q_l}$, for $k \in \{1,\dots,K_1\}$, $l \in \{1,\dots,K_2\}$. The Khatri-Rao product $A * B$ is defined as $(A * B)_{kl} = (A)_{kl} \otimes (B)_{kl}$.

Prepared using rncauth.cls
DOI: 10.1002/rnc

Definition *A.3* (Matrix M)

Define the matrix M as $M \triangleq M_1 * M_2 \in \mathbb{R}^{r\times r}$, where $M_1 \in \mathbb{R}^{r_1\times r_1}$, $r_1 \triangleq 6T$, is block-partitioned into 6×6 T-square blocks, $(M_1)_{kl} \in \mathbb{R}^{T\times T}$, for all $k,l \in \{1,\ldots,6\}$, and $M_2 \in \mathbb{R}^{r_2\times r_2}$, with $r_2 \triangleq 6|\mathcal{G}|$, is block-partitioned into 6×6 square blocks of size $\mathcal{G}$. Let M_1 be defined as $M_1 \triangleq M_1^1 * M_1^2$, where $M_1^1 \triangleq \mathbf{1}_6(\mathbf{1}_6)^\top$ is partitioned in 2×2 blocks, i.e., with 3 block-rows and 3 block-columns, and M_1^2 is the block matrix:

$$M_1^2 = \begin{bmatrix} I_T & I_T & \mathsf{U} \\ I_T & I_T & \mathsf{U} \\ \mathsf{L} & \mathsf{L} & \mathsf{C} \end{bmatrix}, \tag{15}$$

$\mathsf{U} \in \mathbb{R}^T$ is an upper triangular matrix with $\mathsf{U}_{ij} = 1$ for all $i \le j$, i.e., its diagonal entries are also one, $\mathsf{L} \in \mathbb{R}^T$ is a lower triangular matrix with $\mathsf{L}_{ij} = 1$ for all $i \ge j$, $\mathsf{C} = \mathsf{L}\mathsf{U}$. The matrix M_2 is defined as $M_2 \triangleq M_2^1 * M_2^2$, where $M_2^1 \triangleq [\ 1\ \ -1\ \ -1\ \ 1\ \ -1\ \ 1\ ]^\top [\ 1\ \ -1\ \ -1\ \ 1\ \ -1\ \ 1\ ]$ is partitioned into 2×2 blocks, i.e., with 3 block-rows and 3 block columns, and M_2^2 is the block matrix:

$$M_2^2 \triangleq \begin{bmatrix} \frac{2}{U_0^2}W & \cos\theta\mathbf{d}(\Delta V)^{-1} & \cos\theta\mathbf{d}(\beta^{-1}) \\ \cos\theta\mathbf{d}(\Delta V)^{-1} & \frac{U_0^2}{2}\mathbf{d}(\Delta V)^{-1}W^{-1}\mathbf{d}(\Delta V)^{-1} & \frac{U_0^2}{2}\mathbf{d}(\Delta V)^{-1}W^{-1}\mathbf{d}(\beta^{-1}) \\ \cos\theta\mathbf{d}(\beta^{-1}) & \frac{U_0^2}{2}\mathbf{d}(\beta^{-1})W^{-1}\mathbf{d}(\Delta V)^{-1} & \frac{U_0^2}{2}\mathbf{d}(\beta^{-1})W^{-1}\mathbf{d}(\beta^{-1}) \end{bmatrix}. \tag{16}$$

Lemma *A.2* (Positive semidefiniteness of the Khatri-Rao product [13])

Let A, B be compatibly partitioned positive semidefinite symmetric matrices, with square diagonal blocks. Then $A * B$ is positive semidefinite.

Lemma *A.3* (Properties of the matrix M)

For the matrix M in Definition A.3. The following holds:

- M is positive semidefinite,

Prepared using rncauth.cls
DOI: 10.1002/rnc

- null(M) has dimension $4|\mathcal{G}|T$,
- row(M) has dimension $2|\mathcal{G}|T$,
- there is a complete basis for null(M) given by:

$$E \triangleq \begin{bmatrix} I_{|\mathcal{G}|T} & 0 & 0 & 0 \\ I_{|\mathcal{G}|T} & 0 & 0 & 0 \\ 0 & I_{|\mathcal{G}|T} & 0 & \mathsf{U} \otimes (\mathbf{d}(\Delta V)\mathbf{d}(\beta^{-1})) \\ 0 & I_{|\mathcal{G}|T} & 0 & -\mathsf{U} \otimes (\mathbf{d}(\Delta V)\mathbf{d}(\beta^{-1})) \\ 0 & 0 & I_{|\mathcal{G}|T} & -I_{|\mathcal{G}|T} \\ 0 & 0 & I_{|\mathcal{G}|T} & I_{|\mathcal{G}|T} \end{bmatrix}.$$

In the expression above, with some abuse of notation we have omitted for simplicity the dimension of the zero matrix blocks.

Proof

In order to show that M is positive semidefinite, we will show that M_i^j in Definition A.3 is positive semidefinite, for $i, j \in \{1, 2\}$, and we use Lemma A.2 to conclude the result. Note that M_1^1 and M_2^1 are trivially positive semidefinite. Likewise, notice that M_1^2 can be written as $M_1^2 = [\ I_T \quad I_T \quad \mathsf{U}\ ]^\top [\ I_T \quad I_T \quad \mathsf{U}\ ]$. It immediately implies that M_1^2 is positive semidefinite.

In order to show the positive semidefiniteness of M_2^2, we use the Schur complement test. This consists on checking the positive semidefiniteness on one of the Schur complements of the matrix, defined on a block partition of it [14]. Consider the partition of M_2^2 as follows:

$$M_2^2 = \left[\begin{array}{c|cc} \frac{2}{U_0^2}W & \cos\theta \mathbf{d}(\Delta V)^{-1} & \cos\theta(\mathbf{d}(\beta^{-1})) \\ \hline \cos\theta \mathbf{d}(\Delta V)^{-1} & \frac{U_0^2}{2}\mathbf{d}(\Delta V)^{-1}W^{-1}\mathbf{d}(\Delta V)^{-1} & \frac{U_0^2}{2}\mathbf{d}(\Delta V)^{-1}W^{-1}(\mathbf{d}(\beta^{-1})) \\ \cos\theta(\mathbf{d}(\beta^{-1})) & \frac{U_0^2}{2}(\mathbf{d}(\beta^{-1}))W^{-1}\mathbf{d}(\Delta V)^{-1} & \frac{U_0^2}{2}(\mathbf{d}(\beta^{-1}))W^{-1}(\mathbf{d}(\beta^{-1})) \end{array}\right]. \quad (17)$$

Prepared using rncauth.cls
DOI: 10.1002/rnc

We compute the Schur complement of $\frac{2}{U_0^2}W$ in (17). By definition, the Schur complement is:

$$\begin{bmatrix} \frac{U_0^2}{2}\mathbf{d}(\Delta V)^{-1}W^{-1}\mathbf{d}(\Delta V)^{-1} & \frac{U_0^2}{2}\mathbf{d}(\Delta V)^{-1}W^{-1}\mathbf{d}(\beta^{-1}) \\ \frac{U_0^2}{2}\mathbf{d}(\beta^{-1})W^{-1}\mathbf{d}(\Delta V)^{-1} & \frac{U_0^2}{2}\mathbf{d}(\beta^{-1})W^{-1}\mathbf{d}(\beta^{-1}) \end{bmatrix}$$
$$- \frac{U_0^2}{2}\begin{bmatrix} \cos\theta\mathbf{d}(\Delta V)^{-1} \\ \cos\theta\mathbf{d}(\beta^{-1}) \end{bmatrix} W^{-1} \begin{bmatrix} \cos\theta\mathbf{d}(\Delta V)^{-1} & \cos\theta\mathbf{d}(\beta^{-1}) \end{bmatrix} =$$
$$(1-\cos^2\theta)\frac{U_0^2}{2}\begin{bmatrix} \mathbf{d}(\Delta V)^{-1}W^{-1}\mathbf{d}(\Delta V)^{-1} & \mathbf{d}(\Delta V)^{-1}W^{-1}\mathbf{d}(\beta^{-1}) \\ \mathbf{d}(\beta^{-1})W^{-1}\mathbf{d}(\Delta V)^{-1} & \mathbf{d}(\beta^{-1})W^{-1}\mathbf{d}(\beta^{-1}) \end{bmatrix}.$$

Since $1-\cos^2\theta$ is nonnegative, and the matrix above can be expressed as the product of the matrix $\begin{bmatrix} \mathbf{d}(\Delta V)^{-1}W^{-1/2} & \mathbf{d}(\beta^{-1})W^{-1/2} \end{bmatrix}^\top$ times its transpose, we conclude that M_2^2 is positive semidefinite. Since M_i^j are positive semidefinite, for $i,j \in \{1,2\}$, the result follows from Lemma A.2.

Now, let us prove the second, third and fourth bullets.

First let us show that $\operatorname{rank}(M) \geq 2|\mathcal{G}|T$. This follows by the construction of M. Consider a block partition of M in a 6×6 block matrix such that the block columns have $r \times |\mathcal{G}|T$ size. Further, denote the block columns of M as $(M)_j$, for $j \in \{1,\ldots,6\}$. Likewise, denote the block columns of E as $(E)_j$, $j \in \{1,\ldots,4\}$. The block columns $(M)_1$ and $(M)_3$ can be written out as follows:

$$(M)_1 = \begin{bmatrix} I_T \otimes (\frac{2}{U_0^2}W) \\ -I_T \otimes (\frac{2}{U_0^2}W) \\ -I_T \otimes (\cos\theta\mathbf{d}(\Delta V)^{-1}) \\ I_T \otimes (\cos\theta\mathbf{d}(\Delta V)^{-1}) \\ -\mathsf{L} \otimes (\cos\theta\mathbf{d}(\beta^{-1})) \\ \mathsf{L} \otimes (\cos\theta\mathbf{d}(\beta^{-1})) \end{bmatrix}, \quad (M)_3 = \begin{bmatrix} -I_T \otimes (\cos\theta\mathbf{d}(\Delta V)^{-1}) \\ I_T \otimes (\cos\theta\mathbf{d}(\Delta V)^{-1}) \\ I_T \otimes (\frac{U_0^2}{2}\mathbf{d}(\Delta V)^{-1}W^{-1}\mathbf{d}(\Delta V)^{-1}) \\ -I_T \otimes (\frac{U_0^2}{2}\mathbf{d}(\Delta V)^{-1}W^{-1}\mathbf{d}(\Delta V)^{-1}) \\ \mathsf{L} \otimes (\cos\theta\frac{U_0^2}{2}\mathbf{d}(\beta^{-1})W^{-1}\mathbf{d}(\Delta V)^{-1}) \\ -\mathsf{L} \otimes (\cos\theta\frac{U_0^2}{2}\mathbf{d}(\beta^{-1})W^{-1}\mathbf{d}(\Delta V)^{-1}) \end{bmatrix}, \tag{18}$$

Prepared using rncauth.cls
DOI: 10.1002/rnc

Since W^{-1} has rank $|\mathcal{G}|$, then, $I_T \otimes \frac{U_0^2}{2} W^{-1}$ has rank $|\mathcal{G}|T$. This means that $(M)_3$ has rank $|\mathcal{G}|T$. Next, notice that $(I_T \otimes (\frac{U_0^2}{2}\mathbf{d}(\Delta V)^{-1}W^{-1}\mathbf{d}(\Delta V)^{-1}))(I_T \otimes \frac{2}{U_0^2}\cos(\theta)\mathbf{d}(\Delta V)W) = I_T \otimes (\cos\theta \mathbf{d}(\Delta V)^{-1})$. Since $I_\tau \otimes (\frac{U_0^2}{2}\mathbf{d}(\Delta V)^{-1}W^{-1}\mathbf{d}(\Delta V)^{-1})$ is invertible from (18) we can conclude that in order for $(M)_1$ to be linearly dependent of $(M)_3$, $(I_T \otimes (\cos\theta \mathbf{d}(\Delta V)^{-1}))(I_T \otimes \frac{2}{U_0^2}\cos(\theta)\mathbf{d}(\Delta V)W)$ must be equal to $I_\tau \otimes (\frac{2}{U_0^2}W)$. However, it is equal to $I_T \otimes (\cos^2(\theta)\frac{2}{U_0^2}W)$, which means that for $\theta \neq 0$, there is no matrix X such that $(M)_3 X = (M)_1$. Finally, since W is invertible, the rank of $(M)_1$ is equal to $|\mathcal{G}|T$. Then, it follows that $\text{rank}(M) \geq 2|\mathcal{G}|T$.

Now we show that the dimension of $\text{null}(M)$ is at least $4|\mathcal{G}|T$. The reader can verify that the $(M)_j = -(M)_{j+1}$, for $j \in \{1, 3, 5\}$. Therefore it follows that $M(E)_j = 0$, $j \in \{1, \ldots, 3\}$, which means that $(E)_1$, $(E)_2$ and $(E)_3$ are formed by eigenvectors associated with zero eigenvalues. It can also be verified that $(M)_3(\mathsf{U} \otimes (\mathbf{d}(\Delta V)\mathbf{d}(\beta^{-1}))) = -(M)_5$, and $-(M)_3(\mathsf{U} \otimes (\mathbf{d}(\Delta V)\mathbf{d}(\beta^{-1}))) = (M)_6$. Hence, $M(E)_4 = 0$, which means that all columns of $(E)_4$ are eigenvectors of M associated with zero eigenvalues. It is also easy to verify by sparsity of E, that E has full column rank, which means that we have found $4|\mathcal{G}|T$ linearly independent eigenvectors of M with eigenvalue zero. Then, $\text{null}(M)$ has a dimension greater or equal than $4|\mathcal{G}|T$. This, along with the fact that $\text{rank}(M) = 6|\mathcal{G}|T$, ends the proof, since it implies that the sum of $\text{rank}(M)$ and the dimension of $\text{null}(M)$ is greater or equal than r. □

B. PROOF OF THEOREM 3.1

By Lemma 3.1, we have that Algorithm 1 for each node $l \in \mathcal{G}$ is equivalent to the dynamics described by (8), (9), and (10). Therefore, the following analysis is performed directly on these expressions. Let $(q^\star_{\text{in},G}, v^\star, \psi^\star)$ be a fixed point for the algorithm. Existence is guaranteed by assuming that the problem is feasible.

Prepared using rncauth.cls
DOI: 10.1002/rnc

Now, let us show convergence to a fixed point. Let us define variables $y \triangleq q_{\text{in},G} - q^\star_{\text{in},G}$, $z \triangleq v - v^\star$, $\underline{\boldsymbol{\lambda}} \triangleq \underline{\lambda} - \underline{\lambda}^\star$, $\overline{\boldsymbol{\lambda}} \triangleq \overline{\lambda} - \overline{\lambda}^\star$, $\underline{\boldsymbol{\eta}} \triangleq \underline{\eta} - \underline{\eta}^\star$, $\overline{\boldsymbol{\eta}} \triangleq \overline{\eta} - \overline{\eta}^\star$, $\underline{\boldsymbol{\mu}} \triangleq \underline{\mu} - \underline{\mu}^\star$, $\overline{\boldsymbol{\mu}} \triangleq \overline{\mu} - \overline{\mu}^\star$. Further, define $\boldsymbol{\psi} \triangleq \psi - \psi^\star \in \mathbb{R}^r$. Notice that $\boldsymbol{\psi} \triangleq [\overline{\boldsymbol{\lambda}}^\top, \underline{\boldsymbol{\lambda}}^\top, \overline{\boldsymbol{\eta}}^\top, \underline{\boldsymbol{\eta}}^\top, \overline{\boldsymbol{\mu}}^\top, \underline{\boldsymbol{\mu}}^\top]^\top$. After some computations, we obtain that:

$$y^k(t) = -\left(\overline{\boldsymbol{\lambda}}^k(t) - \underline{\boldsymbol{\lambda}}^k(t)\right)\sin\theta, \tag{19}$$

$$\begin{aligned} z^k(t) = &\cos\theta[\overline{\boldsymbol{\lambda}}^k(t) - \underline{\boldsymbol{\lambda}}^k(t)] - \frac{U_0^2}{2} W^{-1}\mathbf{d}(\Delta V)^{-1}[\overline{\boldsymbol{\eta}}^k(t) - \underline{\boldsymbol{\eta}}^k(t)] \\ &- \frac{U_0^2}{2} W^{-1}\sum_{h=t}^{T}\mathbf{d}(\beta^{-1})[\overline{\boldsymbol{\mu}}^k(h) - \underline{\boldsymbol{\mu}}^k(h)]. \end{aligned} \tag{20}$$

Applying the proposed change of variables on the system described by (10), we obtain a dynamics that can be expressed as $\boldsymbol{\psi}^{k+1} = [f_1(\boldsymbol{\psi}^k, y^k, z^k, \psi^\star, q^\star_{\text{in},G}, v^\star)]_+ - [f_2(\psi^\star, q^\star_{\text{in},G}, v^\star)]_+$, for linear maps $f_1 : \mathbb{R}^{2(r+2|\mathcal{G}|T)} \to \mathbb{R}^r$, $f_2 : \mathbb{R}^{2(r+2|\mathcal{G}|T)} \to \mathbb{R}^r$. Notice that y^k and z^k are simply linear functions of $\boldsymbol{\psi}^k$, which do not depend on past values of y, z, hence we can write the dynamics for $\boldsymbol{\psi}$ as $\boldsymbol{\psi}^{k+1} = [f_1(\boldsymbol{\psi}^k, g_1(\boldsymbol{\psi}^k), g_2(\boldsymbol{\psi}^k), \psi^\star, q^\star_{\text{in},G}, v^\star)]_+ - [f_2(\psi^\star, q^\star_{\text{in},G}, v^\star)]_+$, where $g_1 : \mathbb{R}^r \to \mathbb{R}^{|\mathcal{G}|T}$ is given by the right-hand side of (19), and $g_2 : \mathbb{R}^r \to \mathbb{R}^{|\mathcal{G}|T}$ is given by the right-hand side of (20). Then, consider $V(\boldsymbol{\psi}) \triangleq \|\boldsymbol{\psi}\|^2$ as a Lyapunov candidate function that can help us show that all the solutions of the dual decomposition algorithm converge to $\psi^\star$. Moreover, following the same analysis, we show that the fixed point is unique, and by Lemma A.1 we conclude that the optimizer of the problem is unique.

Notice that from the change of variables we introduced above, we have that:

$$\overline{\boldsymbol{\lambda}}^{k+1}(t) = \left[\overline{\lambda}^k(t) + \gamma(w^k_G(t) - W_{\max})\right]_+ - \left[\overline{\lambda}^\star(t) + \gamma(w^\star_G(t) - W_{\max})\right]_+,$$

Prepared using rncauth.cls
DOI: 10.1002/rnc

for all $t \in \tau$. From the non-expansive property of the operator $[\cdot]_+$, i.e., $\|[a]_+ - [b]_+\| \leq \|a - b\|$, we obtain:

$$\|\bar{\boldsymbol{\lambda}}^{k+1}(t)\| \leq \left\| \bar{\boldsymbol{\lambda}}^{k}(t) + \gamma \left(w_G^k(t) - w_G^\star(t) \right) \right\|,$$

for all $t \in \tau$. Further, we replace $w_G^k(t)$ and $w_G^\star(t)$ according to the expression in (5) in order to obtain:

$$\|\bar{\boldsymbol{\lambda}}^{k+1}(t)\| \leq \left\| \bar{\boldsymbol{\lambda}}^{k}(t) + \gamma \left(\frac{2}{U_0^2} \left(\sin\theta W(q_{\text{in},G}^k(t) - q_{\text{in},G}^\star(t)) - \cos\theta W(v^k(t) - v^\star(t)) \right) \right) \right\|.$$

Next, we replace $y^k(t) = q_{\text{in},G}^k(t) - q_{\text{in},G}^\star(t)$ and $z^k(t) = v^k(t) - v^\star(t)$, by the expression in (19), (20), derive the following equation:

$$\begin{aligned} \|\bar{\boldsymbol{\lambda}}^{k+1}(t)\| \leq \Bigg\| \bar{\boldsymbol{\lambda}}^{k}(t) + \gamma \Bigg(& - \frac{2}{U_0^2} W(\bar{\boldsymbol{\lambda}}^{k}(t) - \underline{\boldsymbol{\lambda}}^{k}(t)) \\ & + \cos\theta \left(\mathbf{d}(\Delta V)^{-1} (\overline{\boldsymbol{\eta}}^{k}(t) - \underline{\boldsymbol{\eta}}^{k}(t)) + \sum_{h=t}^{T} \mathbf{d}(\beta^{-1}) (\overline{\boldsymbol{\mu}}^{k}(h) - \underline{\boldsymbol{\mu}}^{k}(h)) \right) \Bigg) \Bigg\|, \end{aligned} \quad (21)$$

for all $t \in \tau$. This procedure can be repeated for $\underline{\boldsymbol{\lambda}}^{k+1}(t)$, $\overline{\boldsymbol{\eta}}^{k+1}(t)$,$\overline{\boldsymbol{\eta}}^{k+1}(t)$, $\overline{\boldsymbol{\mu}}^{k+1}(t)$ and $\underline{\boldsymbol{\mu}}^{k+1}(t)$, for all $t \in \tau$, obtaining:

$$\begin{aligned} \|\underline{\boldsymbol{\lambda}}^{k+1}(t)\| \leq \Bigg\| \underline{\boldsymbol{\lambda}}^{k}(t) - \gamma \Bigg(& - \frac{2}{U_0^2} W(\bar{\boldsymbol{\lambda}}^{k}(t) - \underline{\boldsymbol{\lambda}}^{k}(t)) \\ & + \cos\theta \left(\mathbf{d}(\Delta V)^{-1} (\overline{\boldsymbol{\eta}}^{k}(t) - \underline{\boldsymbol{\eta}}^{k}(t)) + \sum_{h=t}^{T} \mathbf{d}(\beta^{-1}) (\overline{\boldsymbol{\mu}}^{k}(h) - \underline{\boldsymbol{\mu}}^{k}(h)) \right) \Bigg) \Bigg\|, \end{aligned}$$

Prepared using rncauth.cls
DOI: 10.1002/rnc

$$\|\overline{\boldsymbol{\eta}}^{k+1}(t)\| \leq \Bigg\| \overline{\boldsymbol{\eta}}^{k}(t) + \gamma \mathbf{d}(\Delta V)^{-1} \Bigg(\cos\theta(\bar{\underline{\boldsymbol{\lambda}}}^{k}(t) - \underline{\boldsymbol{\lambda}}^{k}(t)) - \frac{U_0^2}{2} W^{-1} \left(\mathbf{d}(\Delta V)^{-1}(\overline{\boldsymbol{\eta}}^{k}(t) - \underline{\boldsymbol{\eta}}^{k}(t)) + \sum_{h=t}^{T} \mathbf{d}(\beta^{-1})(\overline{\boldsymbol{\mu}}^{k}(h) - \underline{\boldsymbol{\mu}}^{k}(h)) \right) \Bigg) \Bigg\|, \tag{22}$$

$$\|\underline{\boldsymbol{\eta}}^{k+1}(t)\| \leq \Bigg\| \underline{\boldsymbol{\eta}}^{k}(t) - \gamma \mathbf{d}(\Delta V)^{-1} \Bigg(\cos\theta(\bar{\underline{\boldsymbol{\lambda}}}^{k}(t) - \underline{\boldsymbol{\lambda}}^{k}(t)) - \frac{U_0^2}{2} W^{-1} \left(\mathbf{d}(\Delta V)^{-1}(\overline{\boldsymbol{\eta}}^{k}(t) - \underline{\boldsymbol{\eta}}^{k}(t)) + \sum_{h=t}^{T} \mathbf{d}(\beta^{-1})(\overline{\boldsymbol{\mu}}^{k}(h) - \underline{\boldsymbol{\mu}}^{k}(h)) \right) \Bigg) \Bigg\|,$$

$$\|\overline{\boldsymbol{\mu}}^{k+1}(t)\| \leq \Bigg\| \overline{\boldsymbol{\mu}}^{k}(t) + \gamma \Bigg(\cos\theta \sum_{h=1}^{T} (\bar{\underline{\boldsymbol{\lambda}}}^{k}(h) - \underline{\boldsymbol{\lambda}}^{k}(h)) - \frac{U_0^2}{2} \mathbf{d}(\beta^{-1}) W^{-1} \sum_{h=1}^{T} \left(\mathbf{d}(\Delta V)^{-1}(\overline{\boldsymbol{\eta}}^{k}(h) - \underline{\boldsymbol{\eta}}^{k}(h)) + \sum_{s=h}^{T} \mathbf{d}(\beta^{-1})(\overline{\boldsymbol{\mu}}^{k}(s) - \underline{\boldsymbol{\mu}}^{k}(s)) \right) \Bigg) \Bigg\|, \tag{23}$$

$$\|\underline{\boldsymbol{\mu}}^{k+1}(t)\| \leq \Bigg\| \underline{\boldsymbol{\mu}}^{k}(t) - \gamma \Bigg(\cos\theta \sum_{h=1}^{T} (\bar{\underline{\boldsymbol{\lambda}}}^{k}(h) - \underline{\boldsymbol{\lambda}}^{k}(h)) - \frac{U_0^2}{2} \mathbf{d}(\beta^{-1}) W^{-1} \sum_{h=1}^{T} \left(\mathbf{d}(\Delta V)^{-1}(\overline{\boldsymbol{\eta}}^{k}(h) - \underline{\boldsymbol{\eta}}^{k}(h)) + \sum_{s=h}^{T} \mathbf{d}(\beta^{-1})(\overline{\boldsymbol{\mu}}^{k}(s) - \underline{\boldsymbol{\mu}}^{k}(s)) \right) \Bigg) \Bigg\|,$$

for all $t \in \tau$. From (21) through (23) we can write $\|\boldsymbol{\psi}^{k+1}\|^2 \leq \|(I_r - \gamma M)\boldsymbol{\psi}^{k}\|^2$, for M as defined in Lemma A.3. It is straightforward to see that the eigenvalues of $I - \gamma M$ are related to the eigenvalues of M as $\lambda_i(I_r - \gamma M) = 1 - \gamma\lambda_i(M)$, where $\lambda_i(M)$ is an eigenvalue of M, with identical eigenvectors, for $i \in \{1, \ldots, r\}$. Then, by Lemma A.3, $I_r - \gamma M$ has $r/2$ eigenvalues 1, with eigenvectors in $\text{null}(M)$. Since M is positive semidefinite, the remaining $r/2$ eigenvalues lie in the interval $[1 - \gamma\rho(M), 1)$. Hence, with $0 < \gamma < \frac{2}{\rho(M)}$, the spectral radius $\rho(I_r - \gamma M) = 1$, but $\lambda_{\max,2} \triangle \max\{\lambda \in \text{spec}(I_r - \gamma M) \mid \lambda \neq 1\}$ is strictly less than one.

Recall that any vector $\boldsymbol{\psi}^{k} \in \mathbb{R}^r$ can be written as unique linear combination $\boldsymbol{\psi}^{k} = \boldsymbol{\psi}^{k}_{\text{row}} + \boldsymbol{\psi}^{k}_{0}$, where $\boldsymbol{\psi}^{k}_{\text{row}} \in \text{row}(M)$, $\boldsymbol{\psi}^{k}_{0} \in \text{null}(M)$ and $\boldsymbol{\psi}^{k}_{\text{row}} \cdot \boldsymbol{\psi}^{k}_{0} = 0$. Therefore, we obtain

Prepared using rncauth.cls
DOI: 10.1002/rnc

$\|\boldsymbol{\psi}^{k+1}\|^2 \leq \|(I_r - \gamma M)(\boldsymbol{\psi}^k_{\text{row}} + \boldsymbol{\psi}^k_0)\|^2$. Since M is symmetric, null(M) and row(M) are invariant under the operator M, hence $(I_r - \gamma M)\boldsymbol{\psi}^k_{\text{row}}$ lies in row(M), and $(I_r - \gamma M)\boldsymbol{\psi}^k_0 = \boldsymbol{\psi}^k_0 \in \text{null}(M)$. By orthogonality of $(I_r - \gamma M)\boldsymbol{\psi}^k_{\text{row}}$ and $\boldsymbol{\psi}^k_0$, it holds that $\|(I_r - \gamma M)(\boldsymbol{\psi}^k_{\text{row}} + \boldsymbol{\psi}^k_0)\|^2 = \|(I_r - \gamma M)\boldsymbol{\psi}^k_{\text{row}}\|^2 + \|\boldsymbol{\psi}^k_0\|^2$. With this result, we have that $\|\boldsymbol{\psi}^{k+1}\|^2 - \|\boldsymbol{\psi}^k\|^2 \leq \|(I_r - \gamma M)\boldsymbol{\psi}^k_{\text{row}}\|^2 + \|\boldsymbol{\psi}^k_0\|^2 - \|\boldsymbol{\psi}^k\|^2 = \|(I_r - \gamma M)\boldsymbol{\psi}^k_{\text{row}}\|^2 - \|\boldsymbol{\psi}^k_{\text{row}}\|^2$. It is well known that the bound $\|(I_r - \gamma M)\boldsymbol{\psi}^k_{\text{row}}\|^2 \leq \lambda^2_{\max,2}\|\boldsymbol{\psi}^k_{\text{row}}\|^2$ holds [15]. Then, we have that $V(\boldsymbol{\psi}^{k+1}) - V(\boldsymbol{\psi}^k) = \|\boldsymbol{\psi}^{k+1}\|^2 - \|\boldsymbol{\psi}^k\|^2 \leq -(1 - \lambda^2_{\max,2})\|\boldsymbol{\psi}^k_{\text{row}}\|^2$. Using LaSalle's invariance principle, we have that any solution of the MICROGRID CONTROL ALGORITHM converges to the largest invariant set contained in null$(M) \cap \{x \in \mathbb{R}^r \mid \|x\| \leq \|\boldsymbol{\psi}^0_0\|\}$.

Next, we show that for any $\psi = \psi^\star + \boldsymbol{\psi}$ such that $\boldsymbol{\psi} \in \text{null}(M)$, it holds that $q_{\text{in},G} = q^\star_{\text{in},G}$, and $v = v^\star$. Notice that if $\boldsymbol{\psi}^k \in \text{null}(M)$, it can be written as $\boldsymbol{\psi}^k = E\boldsymbol{\kappa}^k$, $\boldsymbol{\kappa}^k \in \mathbb{R}^d$, where $d = 4|\mathcal{G}|T$, and E is defined in Lemma A.3. Let us partition the vector $\boldsymbol{\kappa}^k$ according to the block partition of E, as $\boldsymbol{\kappa}^k = [(\boldsymbol{\kappa}^k_1)^\top, (\boldsymbol{\kappa}^k_2)^\top, (\boldsymbol{\kappa}^k_3)^\top, (\boldsymbol{\kappa}^k_4)^\top]^\top$, where we concisely denote $\boldsymbol{\kappa}^k_1 = [\boldsymbol{\kappa}^k_1(1)^\top, \ldots, \boldsymbol{\kappa}^k_1(T)^\top]^\top$, $\boldsymbol{\kappa}^k_2 = [\boldsymbol{\kappa}^k_2(1)^\top, \ldots, \boldsymbol{\kappa}^k_2(T)^\top]^\top$, $\boldsymbol{\kappa}^k_3 = [\boldsymbol{\kappa}^k_3(1)^\top, \ldots, \boldsymbol{\kappa}^k_3(T)^\top]^\top$, and $\boldsymbol{\kappa}^k_4 = [\boldsymbol{\kappa}^k_4(1)^\top, \ldots, \boldsymbol{\kappa}^k_4(T)^\top]^\top$, with $\boldsymbol{\kappa}^k_1(t), \boldsymbol{\kappa}^k_2(t), \boldsymbol{\kappa}^k_3(t), \boldsymbol{\kappa}^k_4(t) \in \mathbb{R}^{|\mathcal{G}|}$, for all $t \in \tau$.

Given the structure of E, it is easy to verify that $\overline{\boldsymbol{\lambda}}^k(t) = \underline{\boldsymbol{\lambda}}^k(t) = \boldsymbol{\kappa}^k_1(t)$, $\overline{\boldsymbol{\eta}}^k(t) = \boldsymbol{\kappa}^k_2(t) + \sum_{h=t}^T \mathbf{d}(\Delta V)\mathbf{d}(\beta^{-1})\boldsymbol{\kappa}^k_4(h)$, $\underline{\boldsymbol{\eta}}^k(t) = \boldsymbol{\kappa}^k_2(t) - \sum_{h=t}^T \mathbf{d}(\Delta V)\mathbf{d}(\beta^{-1})\boldsymbol{\kappa}^k_4(h)$, $\overline{\boldsymbol{\mu}}^k(t) = \boldsymbol{\kappa}^k_3(t) - \boldsymbol{\kappa}^k_4(t)$ and $\overline{\boldsymbol{\mu}}^k(t) = \boldsymbol{\kappa}^k_3(t) + \boldsymbol{\kappa}^k_4(t)$, for all $t \in \tau$. We plug these values in (8) and (9) to obtain:

$$\begin{aligned} q^k_{\text{in},G}(t) &= q_{\text{load},G}(t) + W^{-1}Fq_{\text{load},L}(t) - \sin\theta[\overline{\lambda}^\star(t) + \boldsymbol{\kappa}^k_1(t) - (\underline{\lambda}^\star(t) + \boldsymbol{\kappa}^k_1(t))] \\ &= q^\star_{\text{in},G}(t), \end{aligned}$$

Prepared using rncauth.cls
DOI: 10.1002/rnc

$$
\begin{aligned}
v^k(t) = &- p_{\mathrm{load},G}(t) - p_{\mathrm{in},G}(t) - W^{-1}Fp_{\mathrm{load},L}(t) \\
&+ \cos\theta(\overline{\lambda}^\star(t) + \kappa_1^k(t) - (\underline{\lambda}^\star(t) + \kappa_1^k(t))) \\
&- \frac{U_0^2}{2}W^{-1}\Bigg(\mathbf{d}(\Delta V)^{-1}\Big(\overline{\eta}^\star(t) + \kappa_2^k(t) + \sum_{h=t}^{T}\mathbf{d}(\Delta V)\mathbf{d}(\beta^{-1})\kappa_4^k(h)\Big) \\
&- \mathbf{d}(\Delta V)^{-1}\Big(\underline{\eta}^\star(t) + \kappa_2^k(t) - \sum_{h=t}^{T}\mathbf{d}(\Delta V)\mathbf{d}(\beta^{-1})\kappa_4^k(h)\Big) \\
&+ \sum_{h=t}^{T}\mathbf{d}(\beta^{-1})\left(\overline{\mu}^\star(h) + \kappa_3^k(t) + \kappa_4^k(t) - (\underline{\mu}^\star(h) + \kappa_3^k(t) - \kappa_4^k(t))\right) + \delta c(t)\mathbf{1}\Bigg) \\
= &\, v^\star(t),
\end{aligned}
$$

for all $t \in \tau$. Then, since $\psi^k - \psi^\star \to \mathrm{null}(M)$ as $k \to +\infty$, it follows that $v^k \to v^\star$, $q_{\mathrm{in},G}^k \to q_{\mathrm{in},G}^\star$ as $k \to +\infty$.

REFERENCES

1. J. Carpentier, "Contribution to the economic dispatch problem," *Bulletin de la Societe Francoise des Electriciens*, vol. 3, no. 8, pp. 431–447, 1962.
2. R. A. Jabr, "Radial distribution load flow using conic programming," *IEEE Transactions on Power Systems*, vol. 21, no. 3, pp. 1458–1459, 2006.
3. J. Lavaei and S. H. Low, "Zero duality gap in optimal power flow problem," *IEEE Transactions on Power Systems*, vol. 27, no. 1, pp. 92–107, 2012.
4. J. Lavaei and S. H. Low, "Convexification of optimal power flow problem," in *Allerton Conf. on Communications, Control and Computing*, pp. 223–232, 2010.
5. J. Lavaei, "Zero duality gap for classical opf problem convexifies fundamental nonlinear power problems," in *American Control Conference*, pp. 4566–4573, 2011.
6. K. M. Chandy, S. H. Low, U. Topcu, and H. Xu, "A simple optimal power flow model with energy storage," in *IEEE Int. Conf. on Decision and Control*, pp. 1051–1057, 2010.
7. D. Gayme and U. Topcu, "Optimal power flow with large-scale storage integration," *IEEE Transactions on Power Systems*, vol. 28, no. 2, pp. 709–717, 2013.
8. M. E. Baran and F. F. Wu, "Optimal sizing of capacitors placed on a radial distribution system," *IEEE Transactions on Power Delivery*, vol. 4, no. 1, pp. 735–743, 1989.

Prepared using rncauth.cls
DOI: 10.1002/rnc

9. K. R. C. Mamandur and R. D. Chenoweth, "Optimal control of reactive power flow for improvements in voltage profiles and for real power loss minimization," *IEEE Transactions on Power Apparatus and Systems*, no. 7, pp. 3185–3194, 1981.
10. S. Bolognani and S. Zampieri, "A distributed control strategy for reactive power compensation in smart microgrids," *IEEE Transactions on Automatic Control*, vol. 58, no. 11, pp. 2818–2833, 2013.
11. S. Bolognani, R. Carli, G. Cavraro, and S. Zampieri, "A distributed feedback control strategy for optimal reactive power flow with voltage constraints," *arXiv preprint arXiv:1303.7173*, 2013.
12. A. Cortés and S. Martínez, "Distributed control of reactive power and storage in microgrids," in *Mathematical Theory of Networks and Systems*, (Groningen, The Netherlands), pp. 563–570, July 2014.
13. S. Liu, "Matrix results on the Khatri-Rao and Tracy-Singh products," *Linear Algebra and its Applications*, vol. 289, no. 1, pp. 267–277, 1999.
14. F. Zhang, *The Schur complement and its applications*, vol. 4. Springer, 2005.
15. F. Zhang, *Matrix Theory. Basic Results and Techniques*. Universitext, Springer, second ed., 2011.

Prepared using rncauth.cls
DOI: 10.1002/rnc

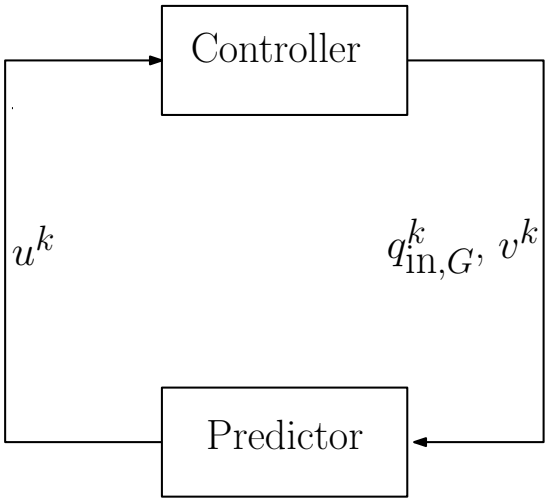

Figure 1. Control computation using voltage prediction.

DOI: 10.1002/rnc

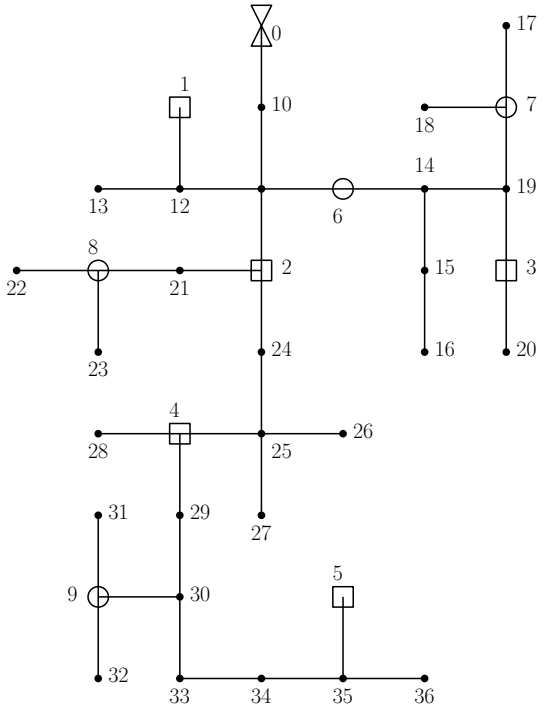

Figure 2. IEEE 37 standard scheme. Squares denote PV generation nodes. Circles denote storage-only nodes.

DOI: 10.1002/rnc

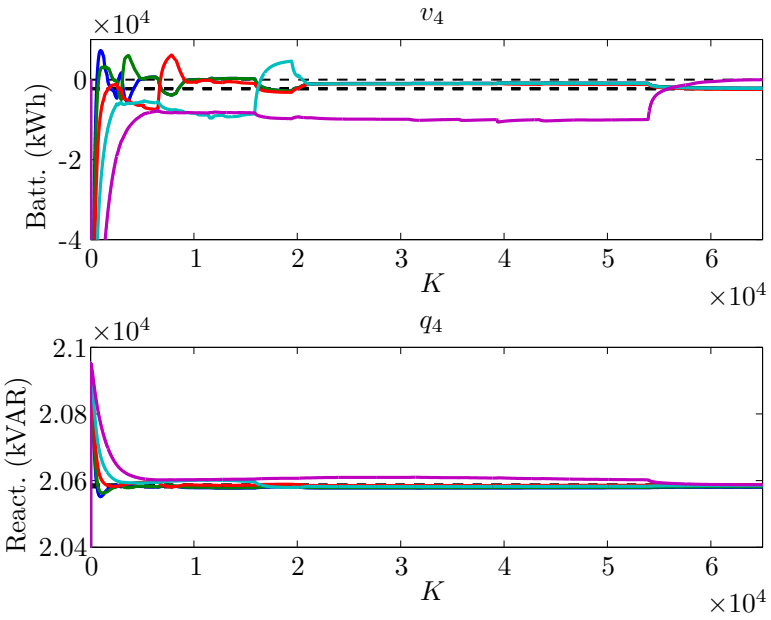

Figure 3. a) Evolution of v_4, b) evolution of q_4, as a function of the iteration number K, respectively, for each $t \in \tau$. Dashed lines show the optimal values.

DOI: 10.1002/rnc

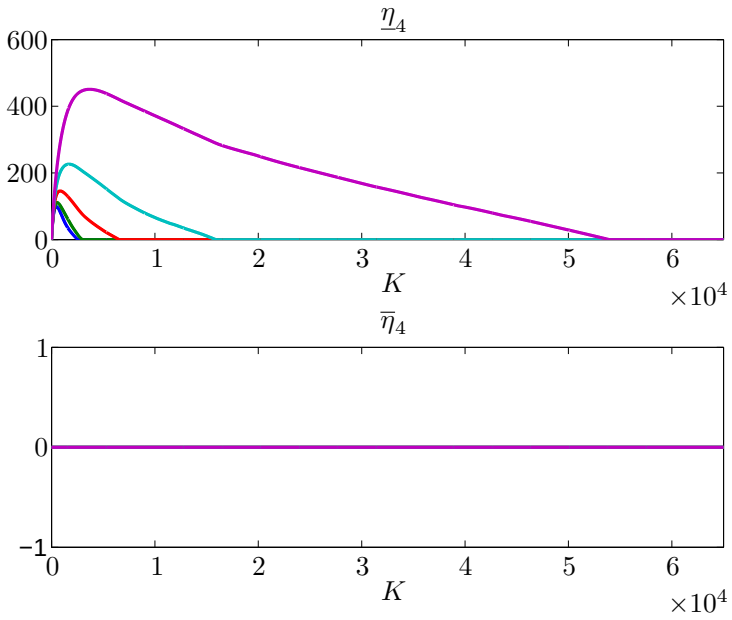

Figure 4. a) Evolution of $\underline{\eta}_4$, b) evolution of $\overline{\eta}_4$ as a function of the iteration number K, respectively, for each $t \in \tau$.

DOI: 10.1002/rnc

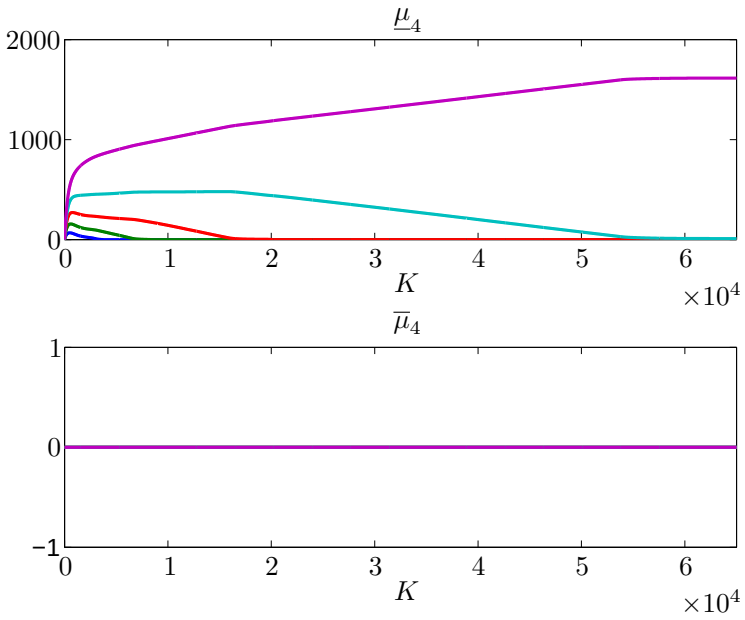

Figure 5. a) Evolution of $\underline{\mu}_4$, b) evolution of $\overline{\mu}_4$ as a function of the iteration number K, respectively, for each $t \in \tau$.

DOI: 10.1002/rnc